AAEC/E498

AAEC/E498

2

# AUSTRALIAN ATOMIC ENERGY COMMISSION

## RESEARCH ESTABLISHMENT

## LUCAS HEIGHTS

DETAILED METEOROLOGICAL INTERPRETATION OF

ACOUSTIC SOUNDER RECORDS

by

G.H. CLARK
E.O.K. BENDUN

February 1981

ISBN 0 642 59709 X

AUSTRALIAN ATOMIC ENERGY COMMISSION
RESEARCH ESTABLISHMENT
LUCAS HEIGHTS

# DETAILED METEOROLOGICAL INTERPRETATION OF ACOUSTIC SOUNDER RECORDS

by

G.H. CLARK
E.O.K. BENDUN

## ABSTRACT

To quantify further the facsimile records from a monostatic acoustic sounder, a series of balloon and near surface meteorological measurements were made in the lower atmosphere under maritime conditions. Tests were concentrated on echo patterns associated with the developing atmospheric mixing layer and arrival of the sea breeze. Similar comparisons were made with an acoustic sounder operating at an inland location with continental climatic conditions. Extrapolation techniques were used to estimate the mixing layer depth between sunrise and initial emergence of the rising echo on the facsimile record. There was reasonable agreement in absolute height and rate of rise of the layer from comparison of the balloon and acoustic sounder measurements. The simple Carson model [D.J. Carson [1973] Q.J.R. Meteorol. Soc., 99:450-467] was also tested to allow extrapolation beyond disappearance of the rising echo. Under sea breeze conditions, the low altitude, elevated echo was associated with a stable temperature profile, a decrease in wind speeds and, frequently, a vertical shear in wind direction to the overlying background flow.

National Library of Australia card number and ISBN 0 642 59709 X

The following descriptors have been selected from the INIS Thesaurus to describe the subject content of this report for information retrieval purposes. For further details please refer to IAEA-INIS-12 (INIS: Manual for Indexing) and IAEA-INIS-13 (INIS: Thesaurus) published in Vienna by the International Atomic Energy Agency.

BALLOONS; METEOROLOGY; TEMPERATURE INVERSIONS; WIND; SURFACE AIR; EARTH ATMOSPHERE; TURBULENCE; RADIOACTIVE AEROSOLS; AIR POLLUTION; DISPERSIONS; PARTICLE RESUSPENSION

CONTENTS



(Continued)

## 1. INTRODUCTION

The AAEC Research Establishment, Lucas Heights, NSW, has been studying the potential of an acoustic sounder to help define the prevailing atmospheric dispersion conditions. From June 1972 to August 1974, an acoustic sounder designed at the RAAF Academy's Physics Department, University of Melbourne, [Shaw 1971] was operated at Jervis Bay in the Australian Capital Territory. Because of the remote location and difficulty in maintenance, instrument performance and data quality were poor. Since October 1975, the acoustic sounder has been relocated at Lucas Heights. This site is approximately 140 m above mean sea level and is located 29 km south-west of Sydney, 18 km west-south-west of Botany Bay and 16 km inland from the Pacific Ocean. Consequently, it is in a maritime environment which has clear diurnal trends in the development of the atmospheric mixing layer as well as the frequent occurrence of a sea breeze later in the day. A short field trip has also been made to Mt Isa in central Queensland where another acoustic sounder is operating under continental climatic conditions.

The acoustic sounders at Lucas Heights and Mt Isa are operated in a monostatic mode, i.e. with transmitter and receiver at the same location, oriented vertically into the atmosphere. With this configuration, back-scattered acoustic echoes are produced by small scale turbulence in the region of larger scale vertical gradients of potential temperature. The echoes are recorded as a shade of grey on the scale black (maximum) through white (zero). The 500 ft* (152.4 m) heights are recorded each 30 min. (1 h for Mt Isa) as the chart travels 2 in. (5.08 cm) per hour. In the monostatic mode, patterns produced by integration of the instantaneous back-scattered echoes do not give quantitative information on such variables as winds and temperatures. However, parameters of importance to atmospheric dispersion predictions may emerge with careful interpretation.

During the early years of acoustic sounder development, much attention was devoted to the detection of atmospheric mixing layer development during the early morning hours [Noonkester 1976; Hall et al. 1975; Shaw 1975]. These studies have shown that a rising echo is associated with a stable, temperature inversion which caps the underlying convectively mixed layer. The movement of the inversion layer has been described theoretically by Carson [1973] and Tennekes [1973] in terms of the diurnal variation of sensible heat input to the convective mixing layer. Studies at Lucas Heights have compared the acoustic sounder echo patterns with theoretical predictions and independent balloon profile measurements.

---

* These acoustic sounders record 500 ft height marks and this is the reason for subsequently using Imperial rather than SI units.

As is the case with the atmospheric mixing layer, the sea breeze is a restriction on pollutant dispersion in the vertical direction [Keen and Lyons 1978]. Bennett and List [1975] speculated that a low altitude, elevated echo which appears on an acoustic sounder after passage of the sea breeze is probably associated with the formation of a mesoscale subsidence inversion. Ahmet [1978] and Lyons [1979] observed similar patterns under sea breezes at other Australian coastal locations. The balloon profile studies at Lucas Heights seek to confirm the presence of a subsidence inversion or wind shear (direction or speed) in the echo region.

In a detailed climatological study of sea breezes in the Sydney region, McGrath [1972] found that sea breezes typically moved across the coastline from an easterly direction and gradually veered to north-east during the day as Coriolis forces became more significant. However, in this study, the definition of a sea breeze did not preclude winds from outside the east to north-east sector and could have included south-east winds if the morning wind was from a non-easterly sector. When the morning wind prevailed from the east, it was necessary to identify changes in the wind speed and turbulence levels to define the arrival of the sea breeze. McGrath [1972] found that although sea breezes were most frequently observed in the summer months (64 per cent of all days on the coast and 55 per cent of those inland), they also occurred during other seasons with different degrees of intensity and inland penetration.

Clark et al. [1977] identified many other different echo patterns to be used in longer term, climatological studies. Because the sea breeze and atmospheric mixing layer regimes produce unique echo patterns, much of the present report is devoted to interpretation of these cases. Other pattern types observed before sunrise and during nocturnal conditions at Mt Isa receive brief mention. The report also discusses detailed interpretation of the acoustic sounder facsimile records in terms of balloon profiles and standard meteorological instrumentation in the lower atmosphere.

## 2. SUPPPORTING METEOROLOGICAL INSTRUMENTATION

The US Nuclear Regulatory Commission (USNRC) has set out guidelines for pre-operational site surveys and on-going surveillance programs at nuclear facilities [e.g. USNRC 1972]; the AAEC has installed special meteorological instrumentation at Lucas Heights following the USNRC guidelines. A meteorological tower (160 ft, 48.8 m) is instrumented at the top with unaspirated wet and dry resistance bulb temperature sensors. Temperature difference between the 30 ft (9.1 m) and 160 ft (48.8 m) levels is measured independently with aspirated resistance bulb sensors. Reliable, good quality data can only be achieved with an on-going calibration program. The wet and dry bulb systems are regularly compared with *in situ* Assmann psychrometer measurements. Since it is difficult to conduct an *in situ* air calibration of the temperature difference system, this is achieved periodically using *in situ* constant temperature water bath techniques.

Wind speed and direction measurements are made using a Dines pressure tube anemograph at 7 m above ground level and a Weather Measure Mark III (WM III) station at 48.8 m. Performance characteristics of the WM III supplied by the manufacturer and the Dines anemograph [Mazzarella 1972] are noted in Table 1. It is obvious that the anemograph is less sensitive to wind turbulence and low wind speeds. Being a cumbersome mechanical device, the Dines is difficult to calibrate in a wind tunnel facility. To overcome this problem, the WM III instrument was initially placed nearby and at the same altitude as the anemograph. Statistics on the responses to mean wind speeds (30 minute manual averages) and turbulence (see Clark and Bendun [1974] for classification of the wind direction turbulence traces) were then compared. These showed that the Dines had a wind speed threshold of 0.9 m $s^{-1}$, underestimated lower speeds, and overestimated higher speeds according to

$$\text{Dines} = 1.2 \times \text{WM III} - 1.1 \ (\text{m s}^{-1}) \quad . \tag{1}$$

This calibration against a secondary standard (WM III) assumes that the latter has a correct factory calibration. In future, the WM III wind speed sensor will be calibrated at regular intervals in the CSIRO Division of Atmospheric Physics' national standards wind tunnel facility.

In addition, net all-wave solar radiation ($\Delta R$) was measured with a polythene shielded Funk [1959] radiometer. This was placed at 0.5 m above a homogeneous, short grass (2-3 cm) surface. An indication of the vertical sensible heat flux into the lower atmosphere is obtained with a Fluxatron [Dyer 1961]. Sensible heat flux is normally written

$$H = \rho C_p \overline{w'T'} \tag{2}$$

where $\rho$ = air density, $C_p$ = specific heat at constant pressure, $w'$ = fluctuation of vertical velocity, $T'$ = fluctuation in ambient temperature, and the overbar denotes a time average. Using pre-determined averaging times, the Fluxatron measures and correlates shorter term fluctuations to give the sensible heat flux. The standard error of sensible heat flux is minimised with longer periods of observation. For a one-hour average, obtained by outputting the instantaneous sensible heat flux data to an integrator, the accuracy is estimated to be 9 per cent [Dyer 1961].

The complex terrain (hills and valleys) and vegetation in the vicinity of Lucas Heights are not ideal for the operation of a Fluxatron. For satisfactory operation, the Fluxatron usually requires a fetch with uniform surface roughness of the order of 100 times the sensor height (in this case 600 m). Alternatively, when there are influences of vegetation (e.g. trees) in the immediate vicinity, another rule of thumb is to place the sensor at at least twice the height of the vegetation.

In view of the uncertainty in the Fluxatron sensor location, an alternative method to estimate H has been proposed. Smith [1972] suggested the following relationship for British conditions:

$$H = 0.4 \times \Delta R + 4.0 \ (\mathrm{mW\ cm^{-2}}) \quad . \qquad (3)$$

Both approaches are used in the following analysis, with the Tennekes [1973] and Carson [1973] atmospheric mixing layer development models, to estimate H for several field study days.

A tethered radiosonde system similar to that described by Morris et al. [1975] was used to measure profiles of meteorological variables to altitudes of the order of 0.8 km above ground level. Wet and dry bulb temperatures (25°C full range with a variable midpoint setting), wind speed (10 m $s^{-1}$ full scale range), wind direction (0 to 360°) and pressure difference (0 to 100 mb*) were telemetered from the balloon to ground level where they were recorded on analogue charts and/or magnetic cassette tapes. Sampling of sensor inputs was continuous, each sensor being monitored sequentially for a one-second interval. The temperatures and wind speeds were scanned once every eight seconds, but pressure difference and wind direction could only be sampled every 16 seconds (i.e. approximately 12-24 m altitude).

Average profiles in Figures 1 to 15 were drawn manually from the instantaneous profiles. Each balloon flight took 30 to 40 minutes for ascent and descent to ground level. The approximate balloon trajectory was plotted as a triangular (pyramidal) line on the acoustic sounder charts. With an evolving and dynamic atmospheric boundary layer, this trajectory enables discontinuities in the meteorological profiles to be compared directly with the occurrence of acoustic sounder echoes.

* millibar (mb) is the standard unit of atmospheric pressure used in meteorology.

# 3. DETAILED INTERPRETATIONS OF LUCAS HEIGHTS ACOUSTIC SOUNDER FACSIMILE RECORDS

## 3.1 Analysis of the Developing Atmospheric Mixing Layer, 20 July 1977

### General description

A strong surface temperature inversion (approximately 5°C per 50 m) developed overnight with light winds from the south and low level intermittent turbulence (trace 6 or 7 - see Clark and Bendun [1974] for this and subsequent references to wind direction turbulence trace types). An anticyclone was centred just west of Sydney and moved overhead during the morning. A gradient wind (see Section 8) from the north-north-west was seen to mix down to ground level after 1200 Eastern Standard Time (EST). The net radiation trace became positive and steadily increased under clear skies after sunrise, which probably occurred just before 0700 EST. Just before sunrise, the acoustic sounder had a type 1 pattern (see Clark et al. [1977] for this and subsequent references to the acoustic sounder pattern recognition scheme). Earlier, at about 0535 EST, a layer was observed to descend (type 11) and merge (type 12) with the surface structure.

### Run 1: 0855 to 0922 EST (see Figure 1)

The balloon profiles indicate a shallow superadiabatic layer (50 m deep) with overlying near-neutral and stable layers. Through the unstable and neutral layers, the southwest winds were light (< 4 m $s^{-1}$) and convective. Within the stable layer above 150 m the wind veered continuously into the northwest sector. The acoustic sounder recorded no evidence of the convective activity near the ground, since it was below the lower limit of instrument detection.

### Run 2: 0923 to 0946 EST

The height of the elevated stable layer rose slowly to about 190 m. At the same time, wind direction shear within the stable layer remained constant at nearly 33° per 100 m. The wind veered through this layer with a constant speed of 5.5 m $s^{-1}$. The echo on the acoustic sounder deepened to a complex type 4.

### Run 3: 0946 to 1016 EST

The acoustic sounder surface echo pattern, which is in transition from type 4 to 5, indicates the first evidence of an intermittent decrease in the intensity of the echoes above the strong (dark) convective echoes near the ground. According to the balloon potential temperature profile, the stable layer had risen to 220 m. Increased turbulence is evident from the fluctuating wind speed and directions within the convective, mixing layer below the stable layer.

Run 4: 1016 to 1037 EST

As the mixing layer developed to a depth of 250 m, the wind direction profile became more uniform from the west. The wind speed averaged 4 m $s^{-1}$ throughout the layer. Broad-based, convective thermal associated echoes can be clearly observed on the acoustic sounder record. The echoes relating to the elevated stable layer are more diffuse.

Run 5: 1056 to 1145 EST

A maximum altitude of 585 m was reached on the final balloon flight. This was sufficient to penetrate the rapidly rising but intermittent echo associated with the base of the stable layer. By the time of this flight the stable layer had risen to 400 m. The last remnants of the rising echo were recorded at 1145 EST at a height of 440 m. The winds from the west-north-west averaged 3.5 m $s^{-1}$ through the atmospheric mixing layer.

## 3.2 Analysis of the Developing Atmospheric Mixing Layer, 21 July 1977

General description

From a complex surface echo pattern (type 3), a double layer echo (type 5) emerged at 0630 EST and persisted until 0930 EST when the surface echo began to rise (type 9). The surface wind direction was consistently turbulent (trace 4) from the south-south-east, although the speed was variable. Initially the synoptic scale gradient wind was from the north at 5 m $s^{-1}$, but by the time of the 1400 EST pibal (pilot balloon flight) it had changed to the west at 6 m $s^{-1}$. After 0800 EST, the wind direction changed to the south-west at 2.4 m $s^{-1}$ as the atmosphere became more unstable.

Run 1: 0919 to 1000 EST (see Figure 2)

This balloon flight corresponded with the initial rise of the surface echo (type 9) and the appearance of lighter echo-free zones below which they were associated with the strengthening convective thermals. The wind speed increased to 6.5 m $s^{-1}$ at the top of the mixing layer while the wind direction slowly reversed from the west to south-west. Within the elevated stable layer, the wind decreased to 2 m $s^{-1}$ at 500 m altitude where there was another increase ($\partial\bar{u}/\partial z > 0$ - see Section 8). The wind then veered to the west-north-west.

Run 2: 1006 to 1048 EST

After the initial rise, the mixing layer depth remained constant at 260 m until 1045 EST. The wind was light and variable from the west-south-west. The position of the low altitude, elevated echo (type 5) was closely related to the location of the base of the stable layer.

Run 3: 1101 to 1139 EST

During this run, the elevated echo rose rapidly, weakened and then disappeared (type 10). Simultaneously, the balloon-borne system measured an increase in depth of the top of the mixing layer, from 290 to 470 m. As a consequence of the convective mixing of the light ground level winds with stronger winds above, the wind speed profiles and surface winds became lighter and more variable (see Figure 2).

Run 4: 1143 to 1207 EST

The solid echo recorded at the apex of the balloon trajectory is due to a direct scattering of sound pulses from the balloon as it drifted over the transceiver. Winds were light and variable through the atmosphere to 420 m. The profiles of potential temperature indicate a near-neutral atmospheric stability. With the disappearance of the elevated echo, broad-based echoes typical of convective thermals (type 13) were observed on the acoustic sounder.

## 3.3 Analysis of the Developing Atmospheric Mixing Layer and Sea Breeze Wind Regime, 16 August 1977

### 3.3.1 The developing atmospheric mixing layer

General description

A strong echo with superimposed waves descended (type 11) from 760 m at about 0030 EST to form a horizontal elevated layer (type 5) at 240 m which persisted until 0500 EST. At this time, the surface layer developed into a homogeneous echo pattern (type 1). Throughout this period a weak inversion (approximately 1.5°C per 100 m) was detected on the meteorological tower. The surface winds were turbulent (trace 4) from the south-west. In the 0900 EST pibal flight, a gradient wind from the south was detected but this changed to a light south-west wind during the afternoon. Under cloudless skies the net radiation began to increase at 0655 EST. With the resulting heat input to the lower atmosphere, conditions became less stable and temperatures began to rise.

Run 1: 0909 to 0941 EST (see Figure 3)

During this balloon flight, the surface echo pattern deepened and became more complex (type 3 or 4). The neutral stability, atmospheric mixing layer developed from 150 to 200 m between the ascent and descent profiles. The elevated stable layer extended to 480 m with a potential temperature gradient of 0.9 K per 100 m. Within the mixing layer there was a strong wind direction shear from west-south-west near the surface to south-south-east above. Winds were light (2 m $s^{-1}$) below the stable layer but increased to 4.5 m $s^{-1}$ above this.

Run 2: 0953 to 1024 EST

The low altitude echo started to rise and separate from the surface (type 9) at 0945 EST. This movement can be clearly correlated with the ascent of the stable layer from 220 to 395 m. Winds in the mixing layer remained light and variable, again backing from the west near the ground to south-south-east at 330 m.

Run 3: 1028 to 1055 EST

The remnants of the rising echo were observed at 1045 EST. The stable layer detected on the ascent potential temperature profile also moved rapidly through 550 m and beyond the peak altitude of this run by the time of descent. Wind speeds were light (3 m $s^{-1}$) and variable throughout the lower atmosphere.

### 3.3.2 The sea breeze wind regime

General description

With the disappearance of the rising echo and further development of atmospheric mixing layer, the near surface winds became light and convective (trace 1). At about 1200 EST, the wind shifted to the south-east sector and, by 1230 EST, there was a stronger wind from the north-east averaging 2.2 m $s^{-1}$. Simultaneously, the net radiometer trace indicated the arrival of broken clouds. Usually the north-east sea breezes observed at Lucas Heights have a higher frequency of turbulence (trace 4), but on this occasion there was also a lower frequency component typical of trace 3.

### Run 4: 1545 to 1620 EST

Elevated patches of echoes which first appeared at 1450 EST were the first indication of the arrival of the sea breeze. The echoes were of weak intensity and varying altitude (type 7). An upper level stable layer at 500 m could have been consistent with the presence of a weak mesoscale subsidence inversion associated with the sea breeze. Within the sea breeze layer, winds were 5 m $s^{-1}$ from the north-north-east.

### Run 5: 1624 to 1712 EST

In addition to the intermittent patches of echoes observed above, a low altitude, elevated echo formed and intensified after 1610 EST. This was directly related to the presence of a stable layer ($\partial\theta/\partial z$ = 0.9 K per 100 m) with increasing wind speeds near its base. The wind changed from the sea breeze direction of east-north-east to north-north-east above 460 m altitude. By the time of balloon descent, the stable layer had extended to near-ground level; the end point of the profile remains elevated because of a transmitter battery pack failure. Simultaneously, the elevated echo descended to the surface to form a complex echo pattern; other intermittent echo patches remained elevated at around 650 m.

## 3.4 Analysis of an On-shore, South-east Wind Regime, 20 April 1978

### General description

During the morning, winds were light and convective with wide low frequency fluctuations generally centred about a northerly direction (see Figure 4). At 1300 EST, the speed increased and wind direction changed to a consistent turbulent (trace 2) wind from the east-south-east. This wind veered slowly to the south-south-east during the early evening. At 7 m altitude, the average speed was 1.8 m $s^{-1}$ during the south-east wind regime. This increased to 4.5 m $s^{-1}$ at 49 m altitude. On the synoptic scale, a weak anticyclone centred to the south caused gradient winds at 5 m $s^{-1}$ to persist from the south to south-south-east all day. The winds at 850 mb (approximately 1500 m) had more of a westerly component. Broken cloud which first appeared at 1010 EST became heavier after 1100 EST. A weak, patchy echo first appeared on the facsimile record soon after 1300 EST, rising initially to 850 m and then slowly descending to 650 m by 1630 EST.

### Run 1: 1647 to 1714 EST

The elevated echo on the acoustic sounder oscillated about 600 m altitude but there was very little near-surface echo structure on the ascent profile.

The appearance of a developing surface echo pattern corresponded to the increasing atmospheric stability during this run. The height of the balloon trajectory was restricted to below 300 m by wind gusts up to 6 m $s^{-1}$ at these altitudes..

Run 2: 1738 to 1813 EST

Strong winds (7 to 8 m $s^{-1}$) prevented the balloon from penetrating the elevated echo at 550 m altitude. The surface echo had developed to a depth of 215 m. A stable potential temperature gradient of 0.65 K per 100 m was established through this layer.

Run 3: 1908 to 1955

Once again strong winds frustrated attempts to reach the elevated echo at 600 m. Through the 150 m deep stable surface layer, winds from the east-south-east had increasing speeds with a shear of 4.4 m $s^{-1}$ per 100 m. This corresponded to a Richardson number of 0.19 which is less than the critical value of 0.25, above which atmospheric turbulence is suppressed. This confirms the observation of a highly turbulent atmosphere prevailing during this balloon flight.

## 3.5 Analysis of the Transition from an On-shore South-east Wind to Nocturnal Regime, 23 June 1978

General description

During the morning, winds prevailed from the south-west with a moderate degree of turbulence (trace 3). At 1445 EST, the wind direction changed to the south-east (trace 2) with a speed of 4 m $s^{-1}$ which slowly abated to 2 m $s^{-1}$ by 1525 EST. Immediately following the wind direction change, the acoustic sounder developed a turbulent echo pattern to 800 m altitude. A low altitude, elevated echo pattern (type 5) emerged, oscillated about 520 m and slowly descended, merging with the surface echo structure at 1730 EST. The wind at 48.8 m changed abruptly from south to west-south-west at 1900 EST with the speed increasing to 4 m $s^{-1}$ (see Figure 5). Nearer the surface, the wind at 7 m was below the threshold of the Dines anemograph and slowly meandered in the south sector until 2015 EST when it became more turbulent from the south-west. An anticyclone with a centre north-west of Sydney caused a gradient flow to persist from the west-north-west between the 1500 and 2100 EST pibal flights.

Run 1: 1942 to 2020 EST

During this flight, the whole layer from ground to 220 m was warmed by an average temperature rise of 3°C. This was apparently caused by the mixing down to ground level of the higher upper wind speeds. The potential temperature gradient changed from 2.49 to 0.98 K per 100 m and the Richardson number from 1.40 to 0.64, which indicated decreasing stability and increasing turbulence in the lower atmosphere. On the acoustic sounder, a low level, transient echo was observed to descend into the surface at about 1930 EST. This might have been associated with the turbulent mixing process. Afterwards a surface echo, with wind speeds reaching 6 m $s^{-1}$ at the top, developed to an altitude of 200 m.

Run 2: 2042 to 2125 EST

Towards the end of this flight (2115 EST) a high level echo first appeared, initially at 750 m and then slowly descending to 550 m by 2230 EST. This could have been caused by a subsidence inversion associated with an anticyclone centred just west of Sydney. Complex surface echo patterns extended beyond the 100 m deep stable layer and region of strong wind shear (4.4 m $s^{-1}$ per 100 m). Wind speeds and potential temperatures were uniform above 100 m. The wind direction was constant from the west-south-west through the entire profile.

Run 3: 2159 to 9999 EST

A transmitter battery pack failure during balloon descent prevented the satisfactory completion of this flight. On ascent, there was a strong stable layer which had redeveloped to 50 m altitude. Again, the wind direction was constant from west-south-west through the entire profile. The lower level echo pattern, which was becoming more diffuse and complex, extended beyond the low level temperature inversion into the neutral layer above.

## 3.6 Analysis of the North-east Sea Breeze Wind Regime, 26 July 1978

General description

During the morning, winds were turbulent (trace 2) with a speed of 4 m $s^{-1}$ (at 48.8 m) from the west direction. Near 1100 EST the speed fell to 2 m $s^{-1}$, turbulence became more convective (trace 3) and the wind veered to the north-north-east. At 1520 EST, a weak east-north-east sea breeze arrived with speeds of 1.4 m $s^{-1}$ at 7 m and 4 m $s^{-1}$ at 49 m altitude. Synoptic scale winds were light (< 4 m $s^{-1}$) throughout the day, with the gradient wind initially in the east-north-east but later veering to the north-north-west as the anticyclone moved from north-east to north-west of Sydney. Initially (1530 EST) the acoustic sounder detected a 600 m deep layer of turbulent air from which a low level elevated echo (type 5) emerged. This persisted until 2120 EST.

Run 1: 1624 to 1701 EST (see Figure 6)

Between 1600 and 1700 EST, the low level echo ascended from 305 to 488 m altitude. On this balloon flight a distinct rise in the stable layer, apparently related to this echo, was detected. On ascent, the stable layer was between 200 and 250 m, and on descent it had risen to span the range 440 to 490 m altitude. Wind speeds decreased from the maximum at the top of the stable layer in both cases. There was no discontinuity in the wind direction profile that could be linked to the stable layer or elevated echo region. Instead it slowly backed from east-north-east near the surface to north at 580 m. It should be noted that a wind from the north preceded the arrival of the sea breeze; this could have been the prevailing macroscale gradient wind.

Run 2: 1753 to 1834 EST

In the lower atmosphere, turbulence became weak and intermittent and the flow was more laminar (Ri = 0.27). At 7 m, the wind speed was below the instrument threshold with a turbulence trace type 7. Higher in the atmosphere (48.8 m) turbulence was even more suppressed (trace 5 or 6) with a constant speed of 4 m $s^{-1}$. A small shear in both the wind speed and temperature above 410 m appeared to be directly related to the weak elevated echo on the acoustic sounder. Nearer the ground, echoes became more complex and patchy with the onset of stable nocturnal conditions.

Run 3: 1906 to 1944 EST

Before this run commenced, the elevated echo had descended and merged with the surface structure leading to identification of a pattern type 4 or 7. In the stable layer, near the ground, flow was laminar (Ri = 0.34), but above 100 m the atmosphere was even more stable with Ri = 2.10. This suppression of atmospheric turbulence corresponded to the region of echo patches on the acoustic sounder and was reflected in the weak northerly winds.

### 3.7 Analysis of the Developing Atmospheric Mixing Layer, 1 August 1978

General description

Before sunrise, winds from the west to north sector were light, with intermittent turbulence and a typical speed of 4 m $s^{-1}$ at 48.8 m. With a tightening pressure gradient ahead of an approaching cold front, the synoptic scale gradient winds were from the west at 3 m $s^{-1}$ (0900 EST), later changing to the north-west at 9 m $s^{-1}$ by 1500 EST. The acoustic sounder detected multiple echoes between 0400 and 0500 EST, including a strong low altitude echo which descended to below 200 m after 0600 EST. Although other intermittent echoes appeared at higher altitudes, it is possible that the stronger echo was still present (embedded in the surface structure) when balloon profiling experiments commenced at 0836 EST. During the morning, incoming solar radiation was restricted by a heavy cloud cover. As a consequence, the atmospheric mixing layer remained very low and did not deepen in the usual manner. From Figure 7, it can be seen that the scale for potential temperature in Run 1 is twice that of subsequent runs.

Run 1: 0836 to 0900 EST

Although the near-ground level winds were light and intermittent (trace 3), there was a strong vertical shear with speeds increasing to in excess of 10 m $s^{-1}$ at 200 m altitude. The largest wind shear coincided with the elevated temperature inversion which had a strong temperature gradient of 6 K per 100 m. There was also a wind direction shear of +44° azimuth per 100 m from west-north-west through this layer. It was not possible to identify a discrete echo at the base of the inversion (150 m) because this was at the lower detection limit of the acoustic sounder in the region of near-ground noise. Strong winds prevented the balloon from penetrating the patchy echo above 400 m.

Run 2: 0909 to 0938 EST

On this run, the balloon was able to penetrate the elevated stable layer into the neutral atmosphere. Near-surface winds veered from north-west to north with moderate turbulence (trace 2) but wind speeds decreased above the layer. The acoustic sounder indicated a type 4 complex surface pattern.

Run 3: 0950 to 1022 EST

The top of the elevated stable layer coincided with the patchy acoustic echo region. There was some unexplained instability in the potential temperature profiles near 200 m which was not reflected in the wind speed and direction profiles. Nearer the surface, north-north-west winds remained light (2.5 m $s^{-1}$ at 48.8 m) with moderate turbulence (trace 2). The effect of the cloud cover was indicated by the very slow deepening of the atmospheric mixing layer. From 0836 to 1022 EST, the layer had only developed from 60 to 140 m (see Figure 7).

Run 4: 1049 to 1116 EST

After 1030 EST, the surface echo structure began to deepen and become patchy near the top, but it maintained a type 4 single layer. Wind speeds above 10 m $s^{-1}$ at 260 m restricted the balloon maximum altitude. At 48.8 m on the tower, the wind speed increased to 4 m $s^{-1}$ and slowly backed into the north-west sector.

## 3.8 Analysis of the Developing Atmospheric Mixing Layer and East-north-east Sea Breeze Wind Regime, 10 October 1978

### 3.8.1 The developing atmospheric mixing layer

General description

During the early morning hours (after 0100 EST), the acoustic sounder detected multiple echoes which descended with time and eventually merged with the surface echo structure. The elevated echo (280 m) observed at 0500 EST (Figure 8) commenced its descent from 550 m at 0130 EST. The lower of the multiple echoes, which merged with the surface echoes (at 305 m) at 0730 EST, was first detected at a height of 1250 m at 0100 EST. The final multiple echo, which merged with the rising echo at 0900 EST, had a similar descent rate (145 m $h^{-1}$).

Nearer ground level, north-west winds had restricted turbulence (trace 7 at 49 m; trace 2 or 8 at 7 m) and a typical speed of 4 m $s^{-1}$ at 49 m. Initially an anticyclone was centred north-east of Sydney but later this weakened and moved south-west, just inland of the coastline. The gradient wind at 6 m $s^{-1}$ changed from north-north-west to west between the 0400 and 0900 EST pibal flights. It was a cloudless morning with sunrise occurring around 0530 EST. There was a constant build-up in sensible heat input to the lower atmosphere after 0600 EST.

Run 1: 0548 to 0618 EST

A strong surface temperature inversion had formed due to radiational and turbulent cooling through the night. This extended 280 m above ground level where there was a sharp discontinuity in the potential temperature profile. A similar shear in the wind speed profile with that of the potential temperature was strongly correlated with the appearance of the elevated echo at 280 m. As seems to be usual with the nocturnal/early morning profiles at Lucas Heights, wind speeds were in excess of 9 m $s^{-1}$ at these altitudes. The wind veered from the west near the ground to be more uniform from the north-west above 180 m.

Run 2: 0630 to 0705 EST

The first influence of heat input into the lower atmosphere can be observed in the potential temperature profiles with a layer of neutral stability extending up to 70 m above ground level; this is well below the lower detection limit of the acoustic sounder. The separate low level echo initially at 280 m merged with the surface echo structure; its influence can be observed as a discontinuity in both the wind speed and potential temperature profiles near 200 m. Two descending echo patterns higher in the atmosphere (at 400 and 600 m) became more intense and were clearly identified during this run. Strong winds prevented further study of these higher echoes.

Run 3: 0759 to 0838 EST

The atmospheric mixing layer which developed to 220 m corresponds with a deepening of the surface echo pattern to 310 m at the top. Lower intermittent echo-free regions were the first indication that the acoustic sounder was able to detect the top of the mixing layer. The balloon profile just reached the base of the descending echo at 510 m but did not measure any discontinuities at this level. Some turbulence was indicated in the wind speed profile above 350 m after speeds decreased through the mixing layer. Winds above the convection layer tended more from the west sector.

Run 4: 0848 to 0922 EST

The balloon was able to reach 560 m altitude under lighter winds. The final descending echo merged with the rising echo pattern (type 9) and a sharp wind shear was observed at this altitude. The rising echo clearly separated from the surface structure and was clearly identified with the position of the elevated stable layer. There were large fluctuations in both wind speed (average 3 m $s^{-1}$) and direction (average north-west) profiles within the mixing layer, but above this the speed increased uniformly to 5 m $s^{-1}$.

Run 5: 0938 to 1015 EST

The rising echo disappeared from the acoustic sounder record during this run. This was probably due to a decrease in the signal-to-noise ratio as it moved out of range. The ascent profile indicated a small stable layer near 460 m which was comparable to the altitude of the rising echo. There were no similar discontinuities in the wind speed and direction profiles at the top of the atmospheric mixing layer.

### 3.8.2 The east-north-east sea breeze wind regime

#### General description

A relative humidity increase of 22 per cent (from 30 per cent initially) accompanied the sea breeze at 1640 EST. Before this, winds had become light and convective from the north-west between 1400 and 1500 EST and then stronger (trace 3) from the south-west. As a consequence of the approximately 100° change in wind direction to the east-north-east, wind speeds decreased to 4 m $s^{-1}$. The gradient wind moved into the west-north-west sector at 7 m $s^{-1}$ during the 1500 EST pibal observation. Unfortunately, the 2100 EST gradient wind data were missing.

#### Run 6: 1639 to 1709 EST (Figure 9)

The start of this run corresponded with the arrival of the sea breeze. Initially the echo structure was not the expected low level, elevated echo pattern (type 5); rather the echoes were complex with patches at all altitudes (type 7). The balloon profiles indicated a depth of 430 m for the sea breeze. With the transition to the south-west above the east-north-east sea breeze layer there was an increase in atmospheric stability and decrease in wind speeds. The balloon profiles indicated better correspondence with the altitude of the surface echo patterns during descent.

#### Run 7: 1724 to 1758 EST

During this run, the near ground level turbulence decreased and wind speeds fell below instrument threshold at 7 m and to 2 m $s^{-1}$ at 48.8 m. Patches of echo-free regions were embedded in the surface pattern on the acoustic sounder. The height of the stable layer appeared well correlated with these echo-free regions, whereas wind direction changes corresponded with the top of the echo structure.

#### Run 8: 1802 to 1829 EST

Elevated patches of echo intensified and were correlated with increased wind speeds and a near neutral to slightly stable atmosphere. Wind directions were variable in this region. The top of the surface echo pattern was associated with wind direction changes and transition from a stable region to near-neutral stability.

## 3.9 Analysis of the Transition from Early Morning to Atmospheric Mixing Layer Development Conditions, 12 October 1978

### General description

After midnight, conditions were typified by a weak surface temperature inversion, low wind speeds from the north-west and intermittent, restricted turbulence (trace 6). Several echoes slowly descended into the surface structure to form three horizontal low altitude layers by 0300 EST (Figure 10). These persisted (intermittently from the middle layer) until 0830 EST. After sunrise (approximately 0530 EST), initial high cloud prevented the normal increase in net radiation until 0650 EST. As a consequence, the input of sensible heat flux to the lower atmosphere and development of the mixing layer were delayed until after 0730 EST; it appears that the Fluxatron may have been out of balance during this period, thus causing low values. Suppression of atmospheric turbulence also continued until after 0715 EST, when the stronger winds higher in the atmosphere were mixed convectively down to ground level. On the synoptic scale, the gradient wind persisted from the north-north-west to north-west sector throughout the day, ahead of a cold front approaching from the south-west.

### Run 1: 0452 to 0530 EST

The balloon was able to reach 460 m altitude, just above the top layer of the multiple echo structure (type 8). The middle layer (base near 260 m) was separated from the surface echo by a very diffuse echo-free region. The lower echo layers were associated with a gradual increase in potential temperature but no marked discontinuities. The wind speed profile was also uniform but there was variability in wind directions throughout the region. The top echo layer coincided with sharp increases in the potential temperature and wind speed.

### Run 2: 0543 to 0622 EST

By contrast with Run 1, the middle echo layer now coincided with significant changes in the meteorological profiles. The wind veered from west-south-west to west, wind speed decreased and there was an increase in atmospheric stability. The top echo layer broadened and became more diffuse. In this region the positive wind shear remained, but the elevated discontinuity in potential temperature disappeared.

Run 3: 0705 to 0747 EST

During this run, convection had just commenced with the atmospheric mixing layer developing from 80 to 130 m. At the top of the surface echo structure (amalgamation of the lower two discrete echoes observed earlier) there was a shear in the gradients of potential temperature and wind direction. The echo-free zone was associated with slight atmospheric stability, uniform wind speed and direction. Through the deep elevated echo (300 to 425 m) there was stronger stability, increasing wind speeds and the wind backed from the west at a rate of 39° azimuth per 100 m.

Run 4: 0800 to 0835 EST

The potential temperature profiles indicated that the mixing layer had developed to 240 m. There was only a slight rise in the top of the surface echo and the elevated echo had become patchy and more diffuse. Wind speeds generally increased with atmospheric stability in this region. The wind from the north-west above the atmospheric mixing layer gradually backed to the west at the top of the profile.

Run 5: 0857 to 0930 EST

An emerging/rising echo pattern (type 9) was indicated by the acoustic sounder. This echo ascended from 250 to 280 m together with the top of the mixing layer. Above this altitude, wind speeds increased with a shear of 2.43 $m\ s^{-1}$ per 100 m, but speeds were light (3 $m\ s^{-1}$) in the lower layers.

Run 6: 0941 to 1022 EST

There were large fluctuations in all meteorological variables throughout the mixing layer. This was most evident near the top of the layer where wind speeds were high (10 $m\ s^{-1}$) and there was a sharp discontinuity in potential temperature. Winds gradually backed from the north near the surface to north-west at 500 m.

Run 7: 1057 to 1137 EST

The rising echo on the acoustic sounder was fading during this balloon flight to 640 m altitude. It could just be related to a discontinuity in the potential temperature profile. The rising echo finally disappeared above an altitude of 850 m at 1110 EST.

## 3.10 Analysis of the Early Morning (Nocturnal) Transition to a Developing Atmospheric Mixing Layer and Onset of the East-north-east Sea Breeze Wind Regime, 21 October 1978

### 3.10.1 Early morning (nocturnal) transition to a developing atmospheric mixing layer

#### General description

The acoustic sounder detected two weak, descending echoes (one with sinusoidal oscillations) at altitudes of 610 and 790 m soon after 0200 EST. The lower echo merged with an ascending layer to form a strong elevated echo at 426 m which persisted until 0750 EST when it was destroyed by the developing atmospheric mixing layer. Between 0400 and 0500 EST there were five horizontal layer echoes (type 8) below 800 m. During this period, near-surface winds were typified by intermittent, low intensity turbulence (trace 6 or 7) and low speeds of the order of 2 m $s^{-1}$. At 7 m, the wind direction was from the south but there was a more easterly component at 49 m. An anticyclone was centred just east of the coastline causing gradient winds from the north-west to north-north-west sectors to persist all day with speeds varying from 3 to 5 m $s^{-1}$. A strong temperature inversion of 2.8°C per 50 m was registered on the meteorological tower during the pre-dawn period, i.e. before 0530 EST.

#### Run 1: 0558 to 0623 EST (Figure 11)

There was considerable variation in the vertical structure of all meteorological variables measured during this run. There was a strong inversion to 40 m above ground level: through this layer the wind direction changed from south-south-east to north; at the top of the layer wind speeds were less than 1 m $s^{-1}$. The wind slowly veered to the north-east at 330 m where there was an increase in speed, rapid turning to the north, and a change in atmospheric stability. These changes corresponded with the passage of the balloon through two elevated echoes at 300 and 370 m. A sharp discontinuity (unstable layer) in the potential temperature on the descent profile, both in this run and in run 2, cannot be explained in terms of acoustic sounder or geophysical observations. Because the wind was generally from the north at higher altitudes, the balloon drifted into the acoustic sounder beam causing a cusp-like reflected echo at the top of the profile. The position of the echo shows excellent agreement in height and time with the independent balloon measurement which is plotted as a triangular trajectory.

## Run 2: 0640 to 0709 EST

The middle elevated echo weakened but the strong upper echo rose and slowly oscillated in height with time. Although not visible as an incipient rising echo on the acoustic sounder, the convection layer deepened from 95 to 150 m during this run. At the top of the surface echo layer, wind speeds began to decrease but there were no changes in the other meteorological variables at this altitude. However, the elevated echo at 430 m was characterised by increased atmospheric stability, wind speeds and a wind direction shear of 56° azimuth per 100 m from the north-east to north-north-west above the echo.

## Run 3: 0748 to 0815 EST

Between runs 2 and 3 the surface echo had started to rise (from pattern 9 to pattern 10) and the elevated echo had merged or been destroyed by the deepening convection (atmospheric mixing) layer. There were large instantaneous fluctuations measured by the balloon package in all variables. However, it did appear that the top of the mixing layer was now near 500 m, an increase of 350 m in 50 minutes. Wind speeds were typically 2.5 m $s^{-1}$ with a veering with height from north at ground level.

## Run 4: 0820 to 0857 EST

A small amount of cloud between 0800 and 0900 EST restricted sensible heat input to the mixing layer which remained at a constant depth. This effect was also seen in the retarded rise of the echo from 426 m at 0800 to 518 m at 0900 EST. At the same time, the balloon profile indicated that the rise was from 480 to 510 m. Winds were light and variable with a turbulence trace 3 near ground level as the speeds began to increase.

## Run 5: 0911 to 0923 EST

This run proved to be a failure when the automatic cutdown device (used only for emergency escape of the balloon) inadvertently activated, puncturing the balloon and causing a premature termination of the flight. As the helium escaped, the balloon's downward trajectory was erratic. This can be seen from the reflected echo on the acoustic sounder facsimile record (Figure 11). This unfortunate incident corresponded with the disappearance of the rising echo at 0935 EST at a height of 700 m. From the balloon profile, it appears that the stable layer at the top of the mixing layer was just identifiable. Winds below 700 m fluctuated about 4 m $s^{-1}$ from the north-north-east.

Run 6: 1030 to 1105 EST

The atmospheric mixing layer extended beyond the acoustic sounder detection range. Through the profile there was neutral stability with winds prevailing from the north-north-west at 4 to 5 m $s^{-1}$ and moderate turbulence (trace 3). It is probable that the reflected acoustic echo from the balloon does not correspond exactly with the plotted balloon trajectory since the balloon was not directly overhead but off the central beam of the acoustic sounder where weaker side lobes provided the acoustic energy for scattering.

### 3.10.2 Onset of the east-north-east sea breeze

General description

Near ground level, winds remained from the north-east to north-north-east sector until 1230 EST, with moderate turbulence (trace 3) and speeds varying from 2 to 5 m $s^{-1}$. There was then a change in direction to the east-north-east accompanied by an increase in turbulence (to trace 2), increased wind speeds of 5 to 6.5 m $s^{-1}$ and a 15 to 50 per cent rise in relative humidity. There was a simultaneous onset of patchy clouds (probably cumulus) which was evident from a fluctuating net radiometer trace. The synoptic scale gradient wind remained in the north-west sector with a speed of 5 m $s^{-1}$. These changes in meteorological variables and observations corresponded with arrival of the sea breeze front. It was not until after 1400 EST that several elevated, patchy echoes were detected on the acoustic sounder. After 1500 EST, a more consistent elevated echo was established.

Run 7: 1350 to 1432 EST (Figure 12)

An unstable layer extending from the ground to 150 m was overlaid with a neutral to slightly stable atmosphere. Although average wind speeds increased to 7 m $s^{-1}$ at the top of the unstable layer from 2 m $s^{-1}$ at ground level, the strong, high frequency turbulence (trace 4) caused marked variability. Winds were mainly from the north-north-east, but backed slightly near the top of the profile.

Run 8: 1519 to 1600 EST

The strong elevated echo was clearly observed between 1500 and 1530 EST at an altitude of 520 m before it rapidly oscillated downwards and then ascended to 460 m at 1535 EST. These balloon profiles were measured during the descent and ascent phase of the echo movement. There is a clear correlation with the movement of the elevated stable layer. Wind speeds also decreased above the top of the sea breeze layer. By contrast with other sea breeze days, when the prevailing gradient wind direction was considerably different to that of the sea breeze, there was only a gradual change of wind to the north-west above the sea breeze layer and not a sharp discontinuity.

Run 9: 1639 to 1723 EST

After the initial period of height oscillations in the elevated echo, it stabilised at 460 m near sunset (approximately 1645 EST) and slowly descended from 1830 EST. Again, there was a clear correlation between the height of the echo and the elevated temperature inversion. Near neutral atmospheric stability was observed in the sea breeze layer.

Run 10: 1750 to 1827 EST

This profile did not penetrate the elevated echo. Winds through the sea breeze layer continued to back slightly from the northeast near the ground to north-north-east at the top. Atmospheric stability was neutral to slightly stable.

## 4. MT ISA ACOUSTIC SOUNDER AND BALLOON METEOROLOGICAL MEASUREMENTS

The Tethersonde balloon system was taken to Mt Isa in central Queensland to study the acoustic sounder performance at an inland location with continental climatic features. Previously, all AAEC balloon profiling experiments had been conducted in the coastal maritime climate of Lucas Heights. The principal aim was to test the universality of a pattern recognition scheme developed by workers at Lucas Heights [Clark et al. 1977] for the long-term interpretation of the acoustic sounder records. Unfortunately, persistent macroscale (synoptic) weather patterns caused meteorological conditions which were unfavourable for balloon flying and the study of a wide range of lower atmospheric and acoustic sounder echo structures.

In an inland desert environment close to tropical regions (latitude 21°S), intense early morning solar radiation causes the rapid removal of the nocturnal surface temperature inversion and development of a deepening atmospheric convection layer. As a consequence, most balloon flights were conducted in nocturnal to early morning conditions when the most interesting phenomena were observed.

The nocturnal profiles were typified by very strong vertical shears of wind speed which frequently restricted the balloon's maximum altitude, generally below the top of the surface echo structure on the acoustic sounder.

Wind shears of 6 m $s^{-1}$ per 100 m altitude were common; these were unsafe for tethered balloon flying.

The acoustic sounder records require only brief comment and interpretation. One exception is a puzzling phenomenon which appeared on several evenings and which is similar to that observed elsewhere [Petersen and Jensen 1976] in the presence of a land breeze. This was designated a 'streaker' echo; it is a very narrow echo (12.5 m thick) which emerged from the surface structure and slowly ascended with time over several hours. Such echoes were observed on the following days (Figures 13 to 15):

| Date | | Time (EST) |
|---|---|---|
| 15 | September 1977 | 1845 to 2200 |
| 16 | | 1950 to > 2300 |
| 18 | | < 0000 to 0500 |

On the latter two evenings, balloon profiles were able to penetrate the low level atmospheric echoes and the incipient streaker echo. Both profiles indicated light southerly winds at ground level (down valley) veering to the south-east at higher altitudes with much higher speeds (8 to 10 m $s^{-1}$). Passing through the region of the streaker echo there appeared to be an increase in turbulent fluctuations of the wind direction; otherwise there were no sharp discontinuities in the profiles which could explain such a specular reflection type echo. From previous observations of the type of patterns observed under sea breeze conditions with a broader, more diffuse echo at the top of the layer, the Mt Isa observations tend to confirm comments by Hall and Neff [1977] on the paper by Petersen and Jensen. They stated that the specular reflection echo was due to non-atmospheric causes and probably was an instrumental or environmental artefact.

Table 2 summarises an interpretation of the Mt Isa acoustic sounder study based on the AAEC pattern recognition scheme [Clark et al. 1977]. Because the balloon flying site was located in a shallow valley where there were large shears of temperatures and winds near the ground, the $\partial\theta/\partial z$ and $\partial\bar{u}/\partial z$ statistics in this table were calculated above 50 m altitude.

## 5. ATMOSPHERIC MIXING LAYER DEVELOPMENT - BALLOON AND ACOUSTIC SOUNDER MEASUREMENTS COMPARED WITH A PRELIMINARY THEORETICAL TREATMENT

The majority of field experiments at Lucas Heights were conducted during the early morning to noon period when the atmospheric mixing layer developed out of the nocturnal structure. This allowed direct comparison of the balloon and acoustic sounder methods for detecting the depth of the mixing layer. In several cases, net all-wave radiation and sensible heat flux measurements were used in the simple model of Carson [1973], which is essentially the same as that of Tennekes [1973], to give an alternative prediction of diurnal changes in the depth of the convective mixing layer.

In Figure 16, the balloon and acoustic sounder measurements are directly compared. The bottom of the rising echo is taken to be the top of the atmospheric mixing layer. This echo height can be estimated from the facsimile records to an accuracy of ± 20 m. It should be noted that there is a time lag between the commencement of convective mixing and its identification, discernible as a rising echo on the acoustic sounder record. This occurs because of a dead-band during pulse transmission (approximate 80 m in the present operational mode) and the usual strong near-ground level echoes associated with the nocturnal echo structure. Consequently, as seen in Figure 16, the acoustic sounder is limited in its mixing layer detection capabilities below approximately 220 m, with the current operating range of 1500 m. One method to overcome this deficiency is linear extrapolation from the time of the first appearance of the rising echo to the time when the net radiation trace starts to increase, i.e. just after sunrise when the mixing layer is at ground level. There is reasonable agreement between the extrapolated and balloon measured curves.

In general, there was good agreement between the balloon and acoustic sounder records both in the absolute height measurements and rate of rise of the atmospheric mixing layer. The largest discrepancies occurred on 12 October 1978 when there was an uneven rate of development, with the stable layer being virtually stationary between 0800 and 0945 EST. This occurred in spite of a steady rise in the net radiation and sensible heat input to the layer (Figure 10). In all cases, there was a slow initial rate of rise which was probably associated with destruction of the stable, nocturnal surface inversion layer. This was followed by a more rapid development when penetrative convection [Tennekes 1973] moves into the layer of less stability.

An inspection of many years of acoustic sounder records has revealed that the rising echo associated with the mixing layer frequently disappears some time during the day. This may be caused by a change in intensity of the elevated stable layer, increased acoustic attenuation as the travel path of the signal becomes longer, or some function of the instrumentation. Whatever the reason, it appears that the acoustic sounder will be useful for measuring the early phases of mixing layer development, but beyond this, theoretical models will be necessary.

The simple model proposed by Carson [1973] requires estimates of the temporal variation of vertical sensible heat input (H) to the layer. Apart from the direct Fluxatron measurements and the Smith [1972] formulations (see Equation 3), reference was made to a study by Oke [1978] in urban/rural areas. At one site, he found that $H = 0.35\ \Delta R$ (mW $cm^{-2}$). The relationships between all three heat flux estimates are indicated in Figure 17. In general, the Smith [1972] approach initially underestimates the heat flux when compared to the Fluxatron; it should be noted that in a more recent article Smith [1979] indicates that his formula has a standard error of 5.5 mW $cm^{-2}$ which is significant at lower values after sunrise. With increasing net radiation values, both the Smith [1972] and Oke [1978] estimates are greater than the Fluxatron measurements.

In Figure 18, the various methods are compared for measurements on 10 October 1978. On this occasion the acoustic sounder did not indicate an echo emerging and rising from the surface structure until 0900 EST at an altitude of 300 m. There was good comparison of the Fluxatron data, balloon measurements and extrapolated acoustic sounder depths until the nocturnal inversion was eroded through a depth of 295 m. The Smith [1972] method underestimated and Oke overestimated depths during this phase; thereafter the Carson model overestimated the rate of rise with all data inputs. However, the Smith [1972] estimates were closest to the acoustic sounder measurements.

On 21 October 1978 the acoustic sounder first indicated the atmospheric mixing layer at 135 m altitude (see Figures 11 and 19). Once again, the Smith [1972] method initially lags because of the heat fluxes shown in Figure 17. There is better agreement between model performances and measurements on this day, especially with the rate of development of the convection layer. It should be emphasised that only the simplest version of the Carson model was tested. No allowance has been made for any larger scale atmospheric subsidence which would decrease the predicted rate of rise, advective or horizontal convective heat losses and mechanical stress factors due to atmospheric turbulence near the ground. More sophisticated models will be tested as they become available.

## 6. CONCLUSIONS

Detailed meteorological interpretations of monostatic acoustic sounder facsimile records have concentrated on unique patterns associated with the developing atmospheric mixing layer during the morning and passage of the sea breeze later in the day. Before a rising echo emerges in the morning (typically at an altitude near 200 m), the acoustic sounder is unable to detect the depth of the mixing layer; extrapolation techniques are required during this period. While the rising echo is present, there is good correlation with the presence of an elevated stable layer, but at some time during the day the rising echo frequently disappears and the acoustic sounder again loses its ability to detect the atmospheric mixing layer. The simple Carson model was tested against simultaneous balloon and acoustic sounder measurements with a view to using the results to extrapolate beyond the time when the rising echo faded. There was reasonable agreement, but more work is required to account for other influences using more sophisticated models.

After the passage of a sea breeze the acoustic sounder detects a low altitude, elevated echo. Balloon measurements indicated that this echo was associated with a stable, temperature inversion, a decrease in wind speed from the stronger sea breeze below, and often a wind direction shear. A vertical wind direction shear at the top of the sea breeze layer is dependent on the prevailing wind direction before the sea breeze incursion. Most of the sea breezes were from the east to north-east direction. Attempts were made to investigate south-east winds which also have a cross-coastline trajectory and similar echo patterns. However, the elevated echoes were higher, and stronger winds prevented the balloon from reaching these altitudes.

Both the atmospheric mixing and sea breeze layers are important restrictions on the vertical dispersion of atmospheric pollutants owing to the presence of the elevated stable layer. Because they could be uniquely defined on the acoustic sounder facsimile records they were the subject of these initial balloon meteorological measurements. In future the more complex acoustic sounder patterns which were identified by Clark et al. [1977] will be studied intensively to further investigate the potential of this instrument in air pollution meteorology.

## 7. ACKNOWLEDGEMENTS

The assistance of Dr I. Bourne of the RAAF Physics Department, University of Melbourne was vital in occasional times of crisis during the long-term operation of the acoustic sounder. Mt Isa Mines personnel provided fine facilities during our collaborative research studies. Mr J. Kristo did an excellent job in collating and preparing the diagrams, and Mrs C. Chrimes made a similar contribution in typing from the manuscript. We gratefully acknowledge all of this assistance.

## 8. GLOSSARY

$\theta$ Potential temperature (K)

$\partial\theta/\partial z$ Vertical gradient of potential temperature (a measure of atmospheric stability).

$< 0$ Unstable atmospheric stability - superadiabatic

$= 0$ Neutral atmospheric stability - adiabatic

$> 0$ Stable atmospheric stability

$\bar{u}$ Mean horizontal wind speed

$\partial\bar{u}/\partial z$ Vertical gradient of mean wind speed

$Ri = g(\partial\theta/\partial z) \Big/ (\partial\bar{u}/\partial z)^2$ = Richardson number

g = Gravitational acceleration constant

Backing wind - an anticlockwise change of wind direction

Veering wind - a clockwise change of wind direction

Gradient wind - air motion parallel to the isobars; in this case taken as the 900 mb (approximately 1030 m) wind from the pilot balloon (pibal) flights at Sydney (Mascot), some 20 km to the east-north-east of Lucas Heights.

## 9. REFERENCES


Ahmet, S. [1978] - Development of acoustic sounding technique for operational use. Australian Department of Science, Bureau of Meteorology, Meteorological Study No.29.

Bennett, R.C. and List, R. [1975] - Lake breeze detection with an acoustic sounder. Proc. 16th Conf. on Radar Meteorol. of the American Meteorol. Soc., Houston, Texas, 22-24 April, pp.253-256.

Carson, D.J. [1973] - The development of a dry inversion-capped convectively unstable boundary layer. Q.J.R. Meteorol. Soc., 99(421)450-467.

Clark, G.H. and Bendun, E.O.K. [1974] - Meteorological research studies at Jervis Bay, Australia. AAEC/E309.

Clark, G.H., Charash, E. and Bendun, E.O.K. [1977] - Pattern recognition studies in acoustic sounding. J. Appl. Meteorol., 16(12)1365-1368.

Dyer, A.J. [1961] - Measurements of evaporation and heat transfer in the lower atmosphere by an automatic eddy-correlation technique. Q.J.R. Meteorol. Soc., 87(373)401-412.

Funk, J.P. [1959] - Improved polythene shielded net radiometer. J. Sci. Instrum., 36(6)267-270.

Hall, F.F., Edinger, J.G. and Neff, W.D. [1975] - Convective plumes in the planetary boundary layer, investigated with an acoustic sounder. J. Appl. Meteorol., 14(4)513-523.

Hall, F.F. and Neff, W.D. [1977] - Comments on 'A mesoscale phenomenon revealed by an acoustic sounder'. J. Appl. Meteorol., 16(1)109-110. (See Petersen and Jensen [1976]).

Keen, C.S. and Lyons, W.A. [1978] - Lake/land breeze circulations on the western shore of Lake Michigan. J. Appl. Meteorol., 17(12)1843-1855.

Lyons, T. [1979] - personal communication.

McGrath, C.A. [1972] - The development of the sea breeze over Sydney and its effect on climate and air pollution. M.Sc. thesis, School of Earth Sciences, Macquarie University, Australia.

Mazzarella, D.A. [1972] - An inventory of specifications for wind measuring instruments. Bull. Am. Meteorol. Soc., 53(9)860-871.

Morris, A.L., Call, D.B. and McBeth, R.B. [1975] - A small tethered balloon sounding system. Bull. Am. Meteorol. Soc., 56(9)964-969.

Noonkester, V.R. [1976] - The evolution of the clear convective layer revealed by surface-based remote sensors. J. Appl. Meteorol., 14(6)67-77.

Oke, T.R. [1978] - Surface heat fluxes and the urban boundary layer. WMO Symposium on Boundary Layer Physics Applied to Specific Problems of Air Pollution, Norrköping, 19-23 June. WMO-No.510.

Petersen, E.L. and Jensen, N.O. [1976] - A mesoscale phenomenon revealed by an acoustic sounder. J. Appl. Meteorol., 15(6)662-664.

Shaw, N.A. [1971] - Acoustic sounding of the atmosphere. Ph.D Thesis, Dept. of Physics, RAAF Academy, University of Melbourne, Australia.

Shaw, N.A. [1975] - Observations of atmospheric structure using an acoustic sounder. ANL/RER/75-2.

Smith, F.B. [1972] - A scheme for estimating the vertical dispersion of a plume from a source near ground level. Proc. Third Meeting of the Panel on Air Pollution Modelling, NATO/CCMS, Paris, N.14.

Smith, F.B. [1979] - The relation between Pasquill stability p and Kazanski-Monin μ (in neutral and unstable conditions). Atmos. Env., 13(6)879-881.

Tennekes, H. [1973] - A model for the dynamics of the inversion above a convective boundary layer. J. Atmos. Sciences, 30(4)558-567.

USNRC [1972] - Regulatory Guide 1.23 (Safety Guide 23), 'On-site Meteorological Programs', US Nuclear Regulatory Commission, Washington, D.C.

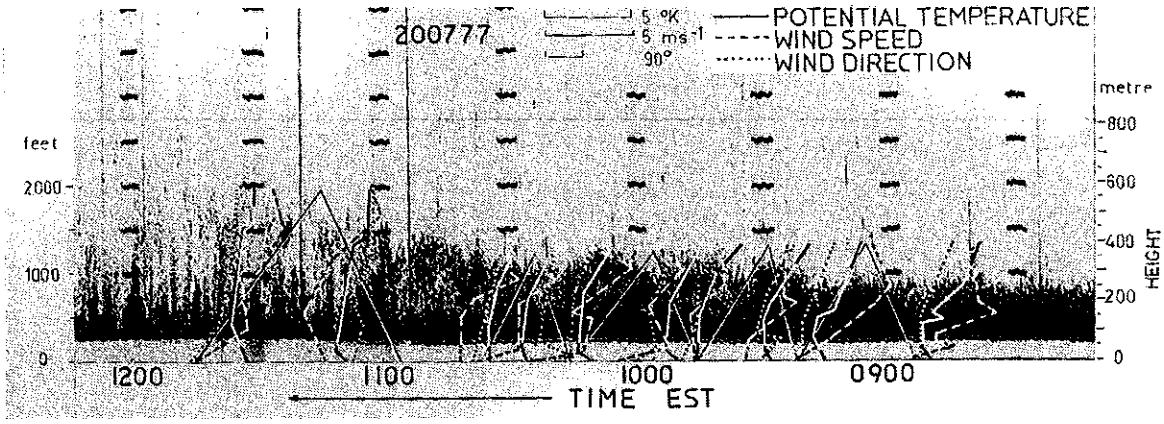


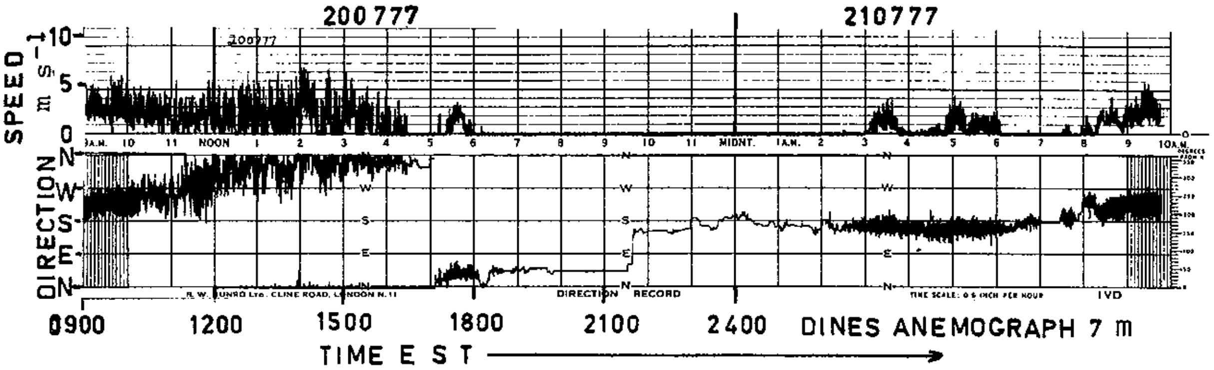


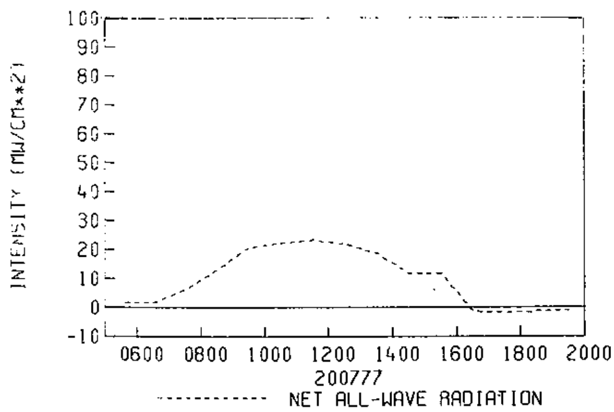


**FIGURE 1. METEOROLOGICAL AND ACOUSTIC SOUNDER DATA, 20 JULY 1977**

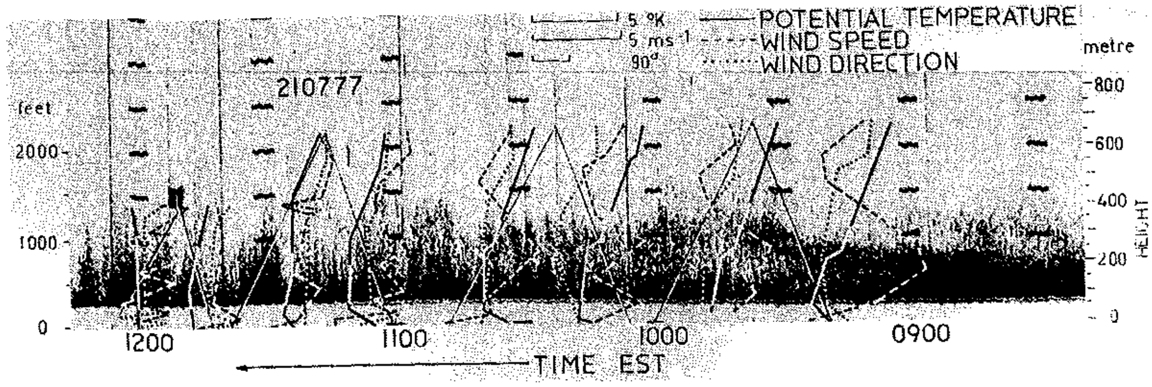


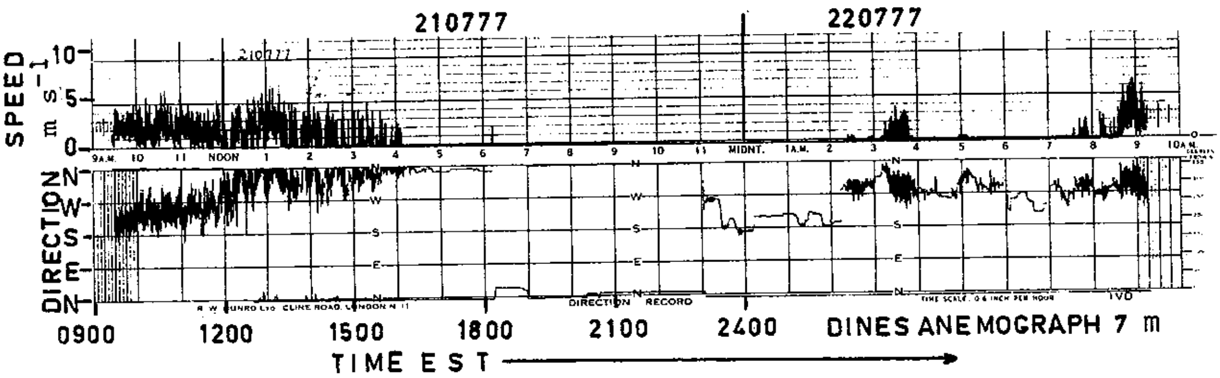


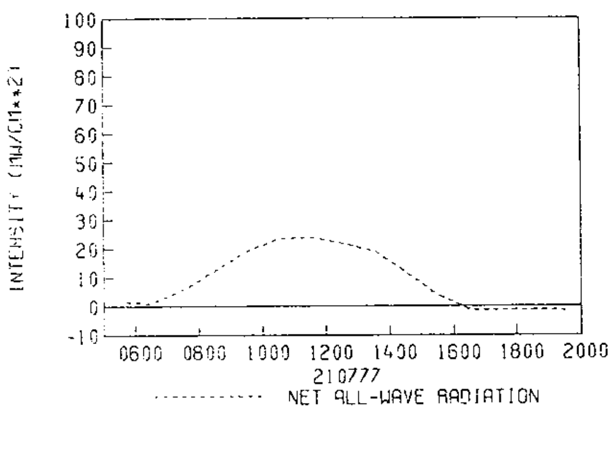


**FIGURE 2. METEOROLOGICAL AND ACOUSTIC SOUNDER DATA, 21 JULY 1977**

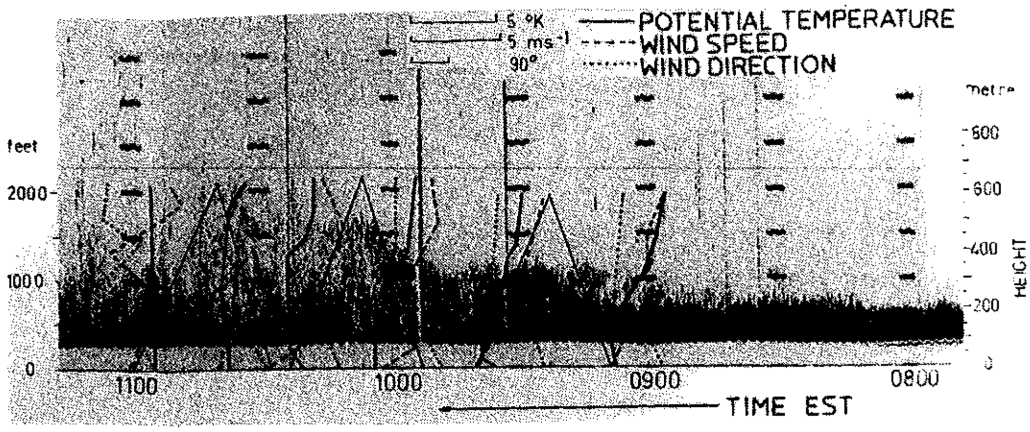


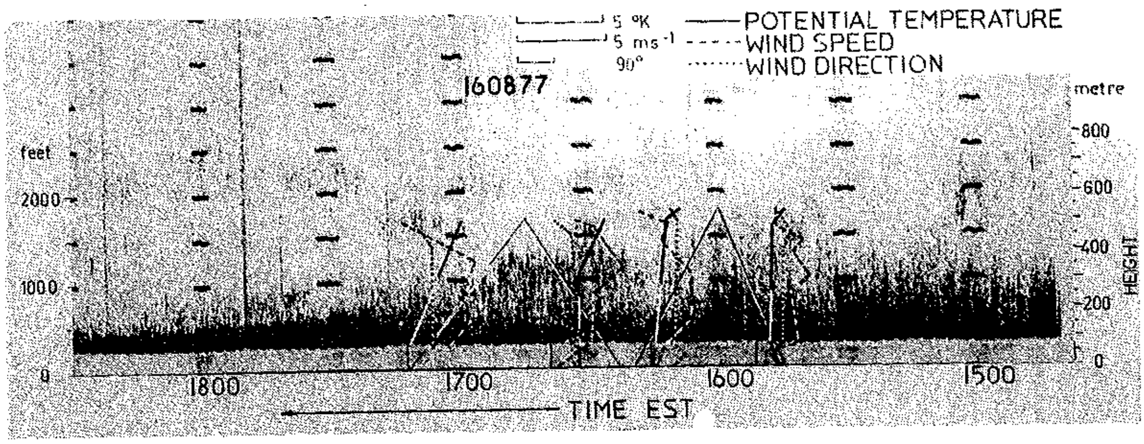


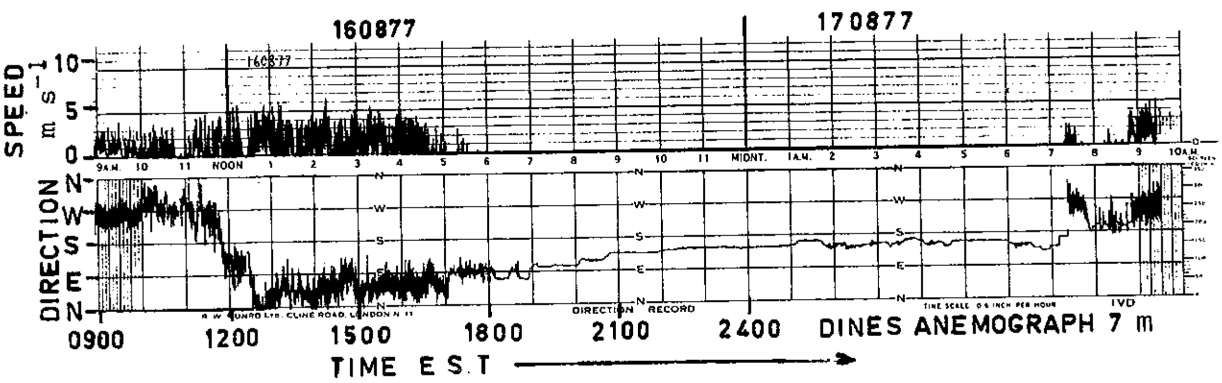


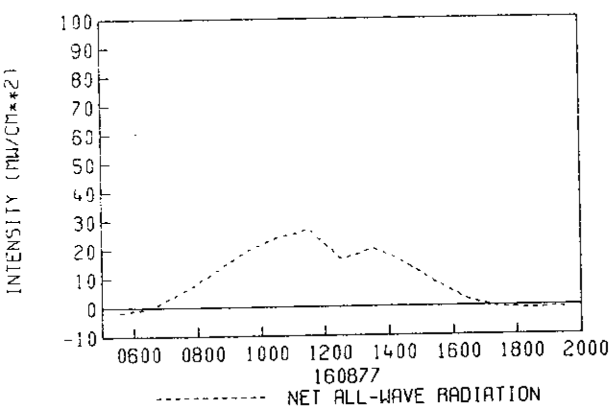


**FIGURE 3. METEOROLOGICAL AND ACOUSTIC SOUNDER DATA, 16 AUGUST 1977**

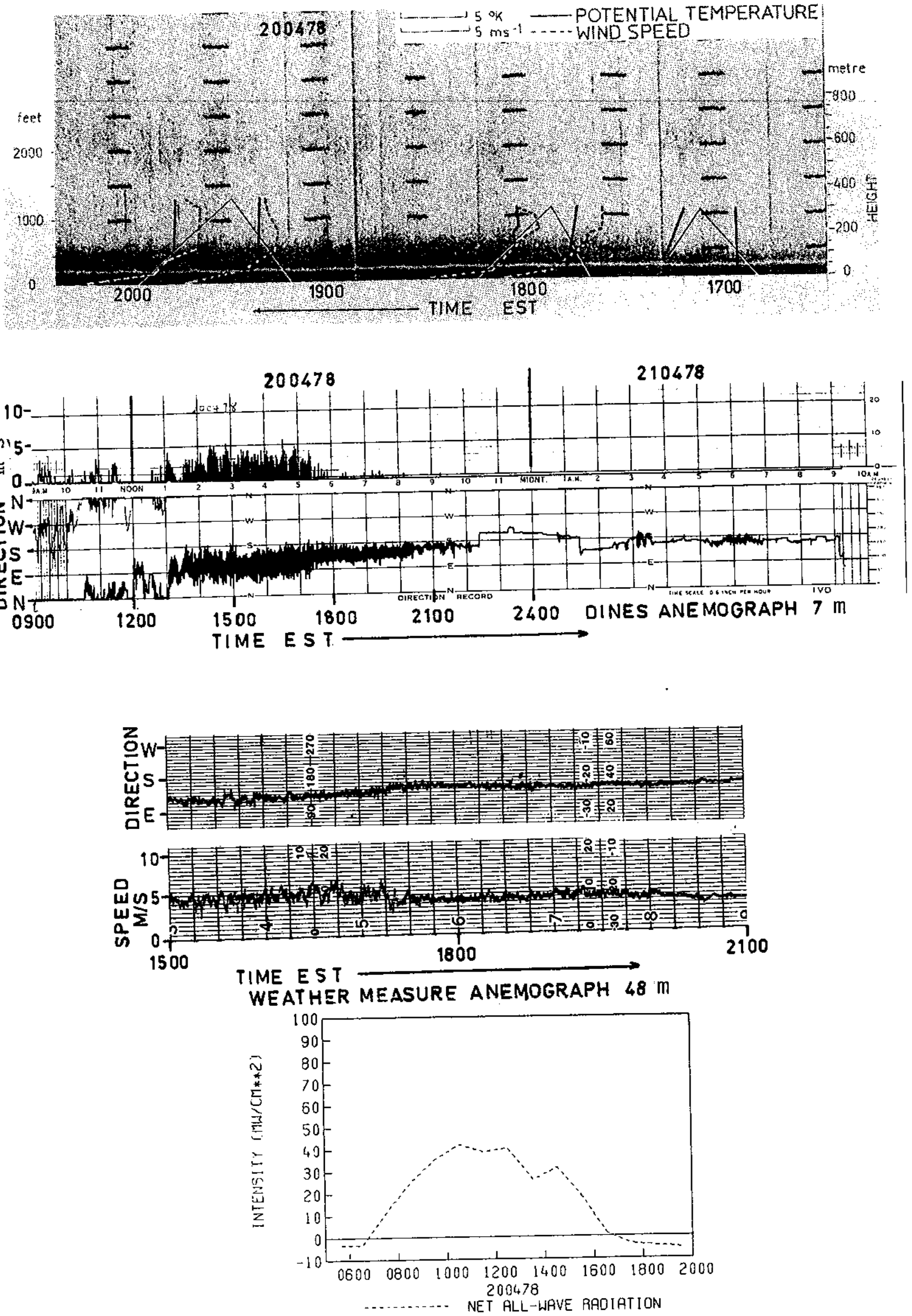


**FIGURE 4. METEOROLOGICAL AND ACOUSTIC SOUNDER DATA, 20 APRIL 1978**

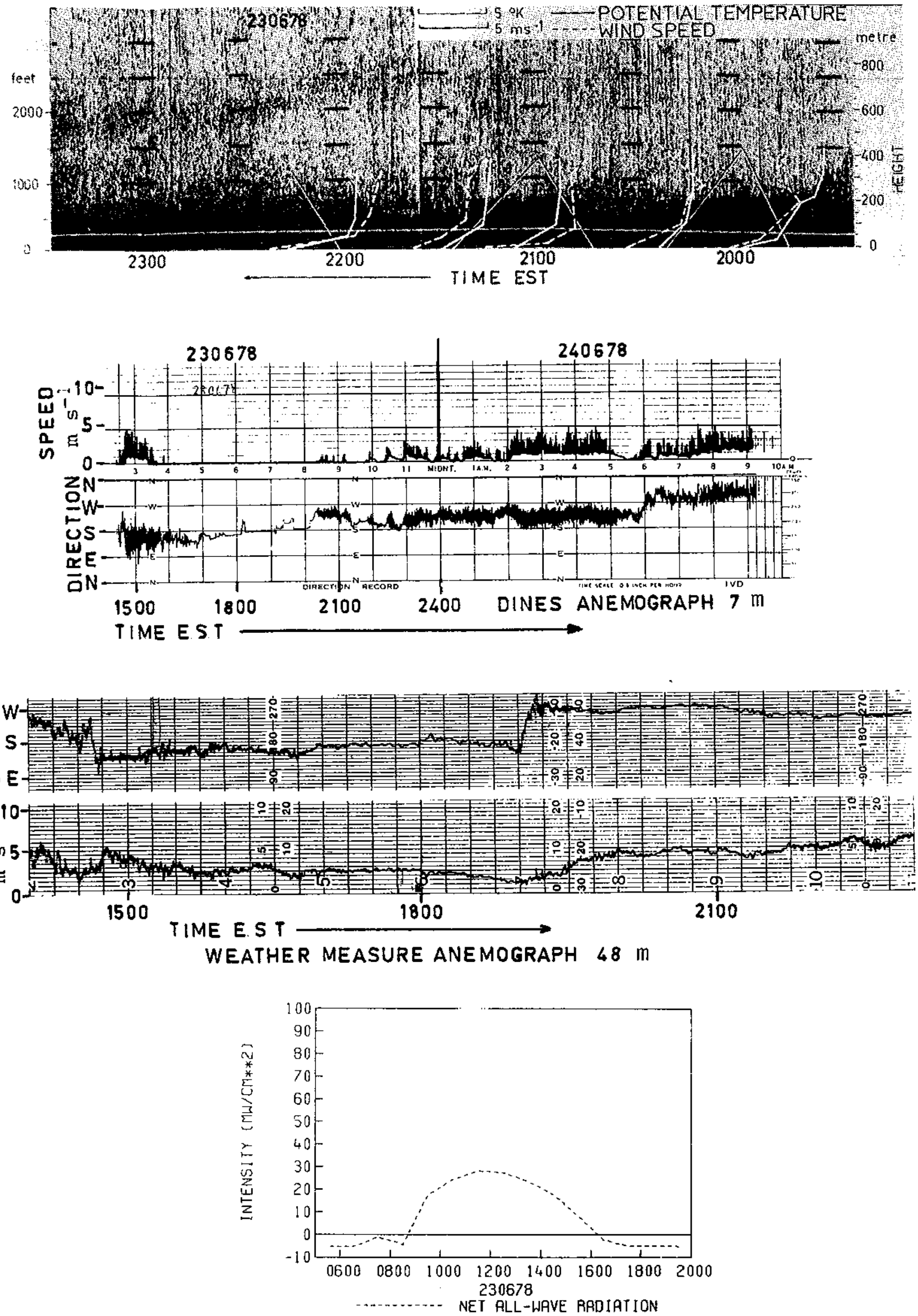


**FIGURE 5. METEOROLOGICAL AND ACOUSTIC SOUNDER DATA, 23 JUNE 1978**

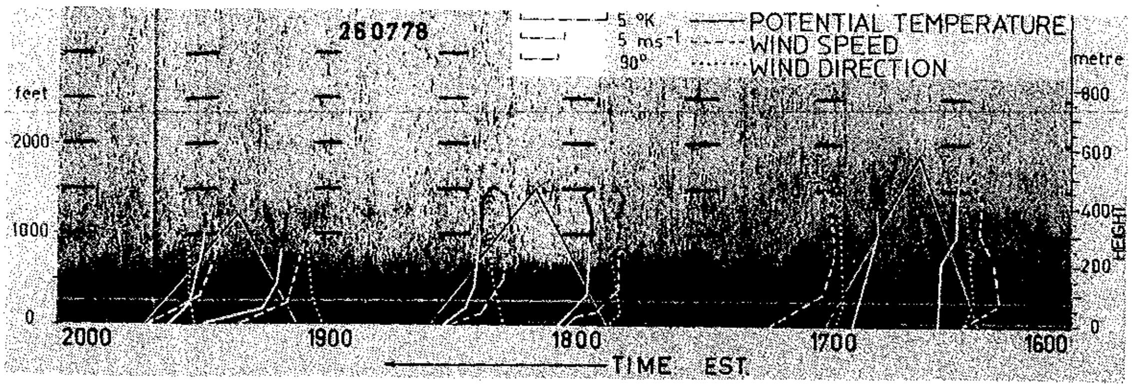


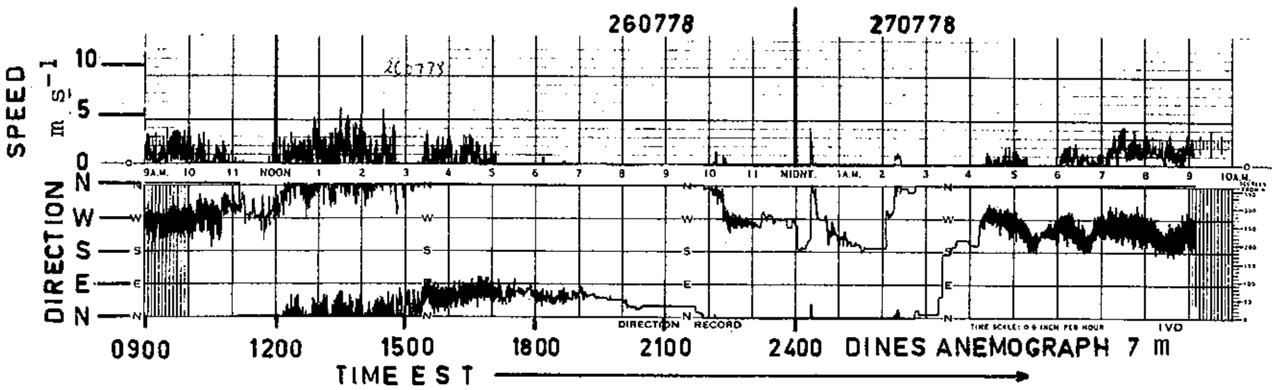


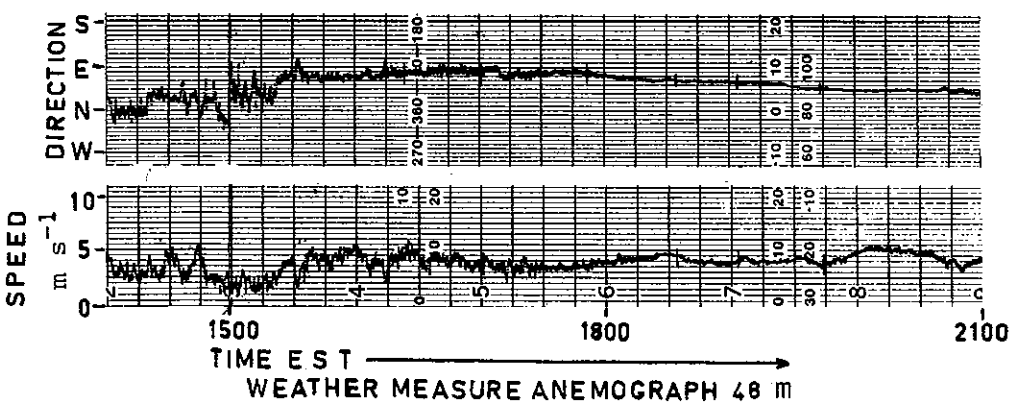


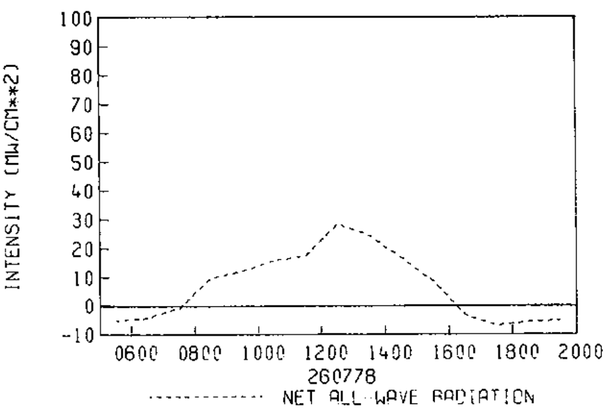


**FIGURE 6. METEOROLOGICAL AND ACOUSTIC SOUNDER DATA, 26 JULY 1978**

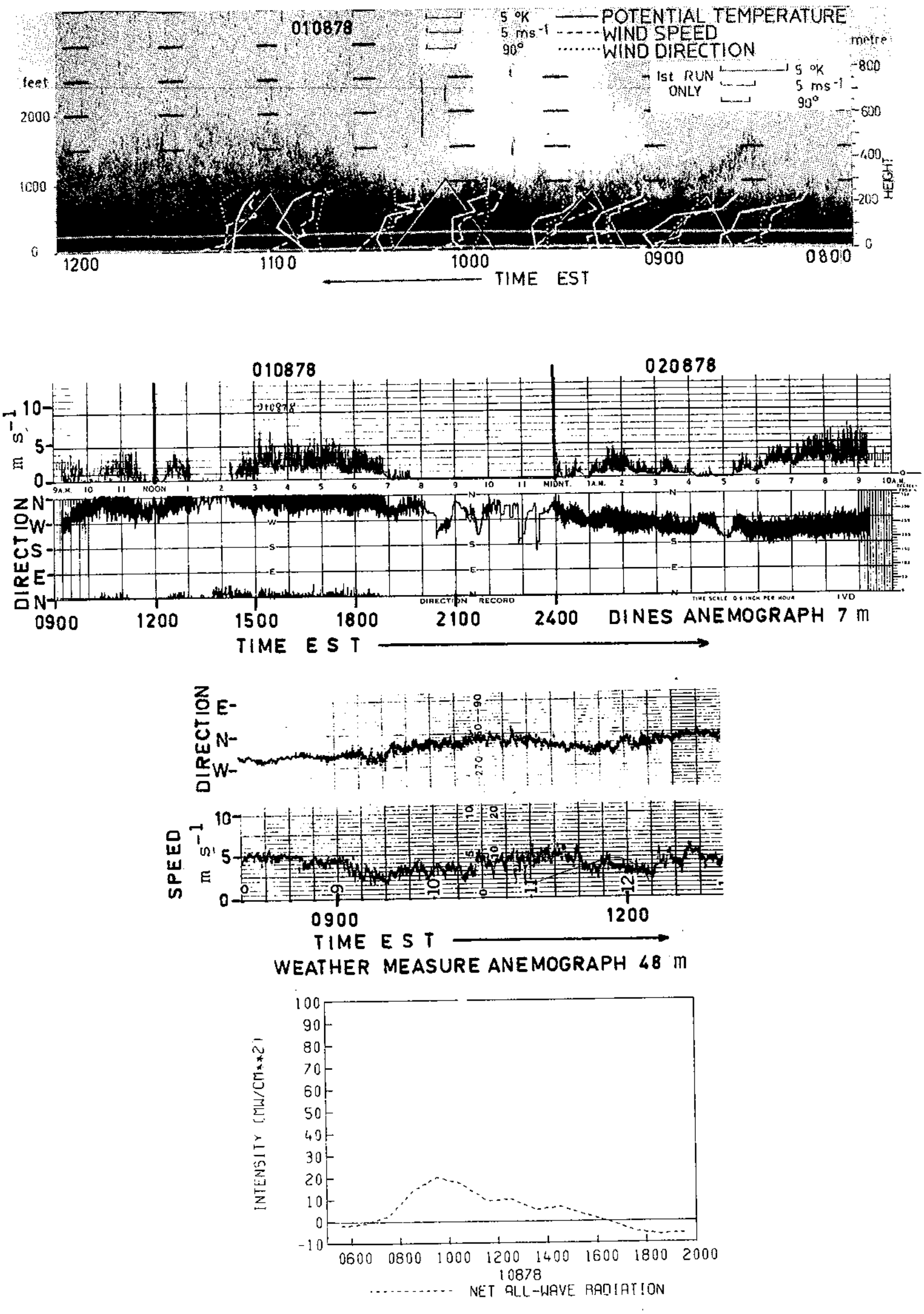


**FIGURE 7. METEOROLOGICAL AND ACOUSTIC SOUNDER DATA, 1 AUGUST 1978**

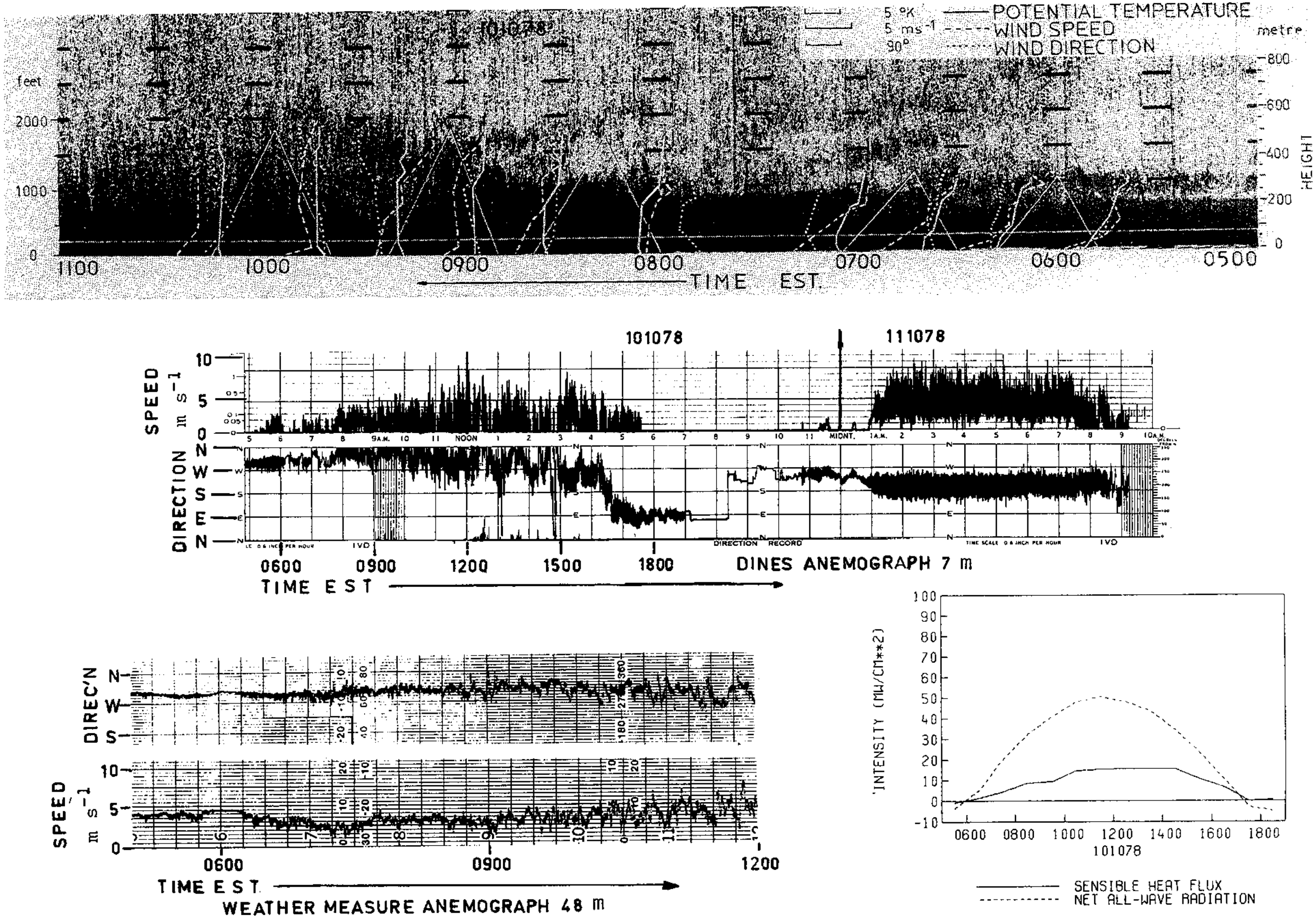


**FIGURE 8. METEOROLOGICAL AND ACOUSTIC SOUNDER DATA - ATMOSPHERIC MIXING LAYER DEVELOPMENT 10 OCTOBER 1978**

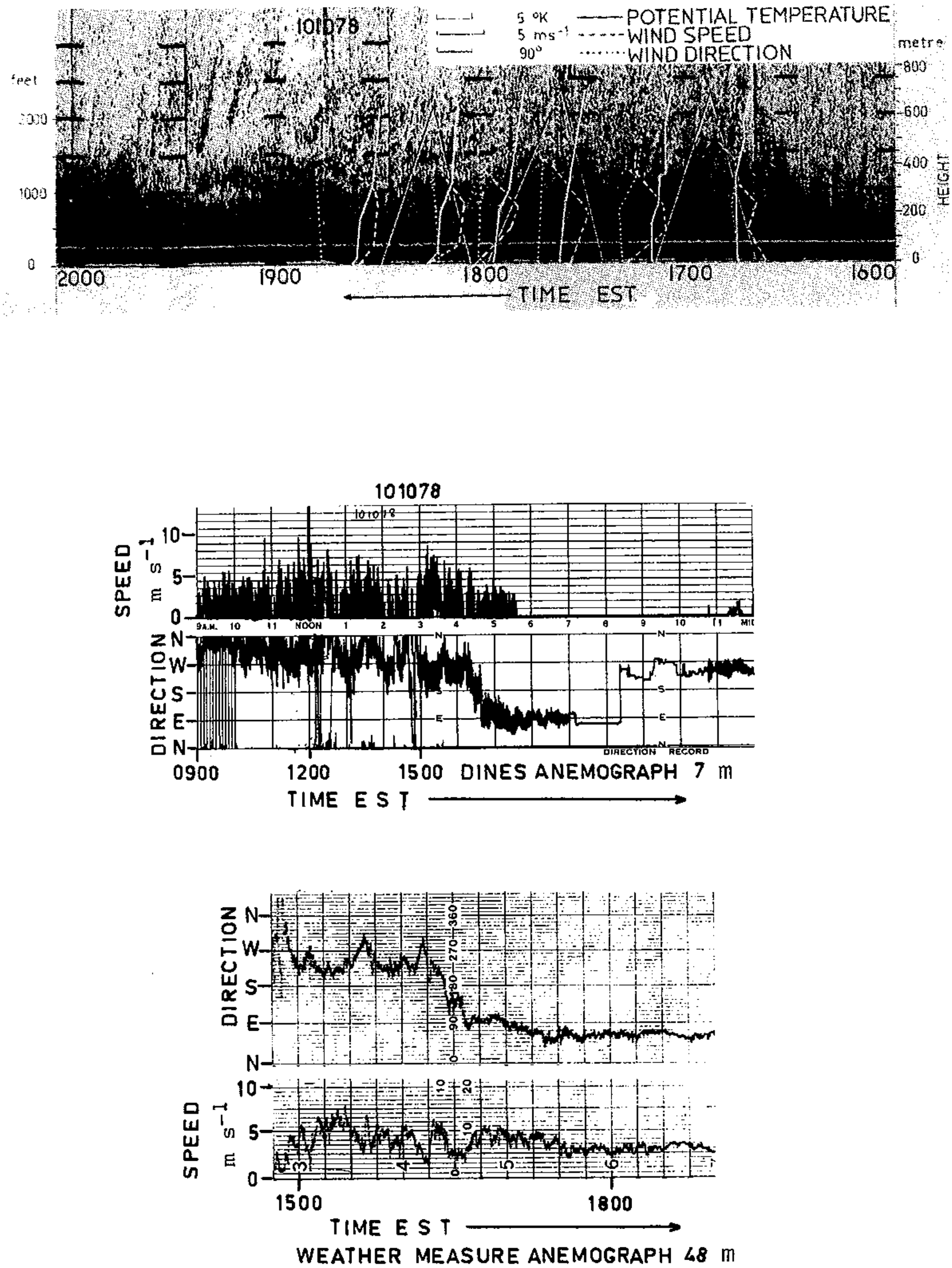


**FIGURE 9. METEOROLOGICAL AND ACOUSTIC SOUNDER DATA - EAST-NORTH-EAST SEA BREEZE WIND REGIME, 10 OCTOBER 1978**

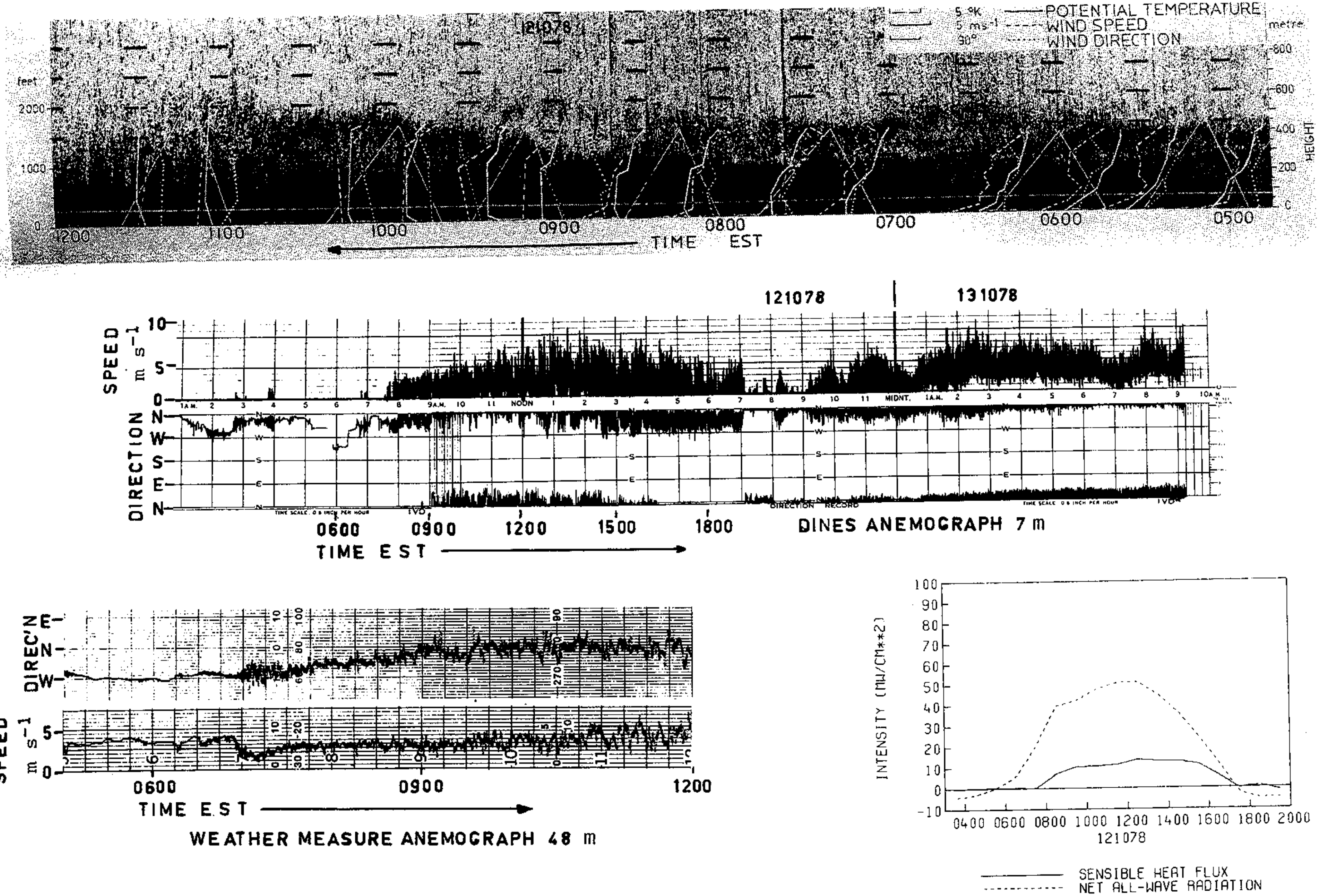


**FIGURE 10. METEOROLOGICAL AND ACOUSTIC SOUNDER DATA, 12 OCTOBER 1978**

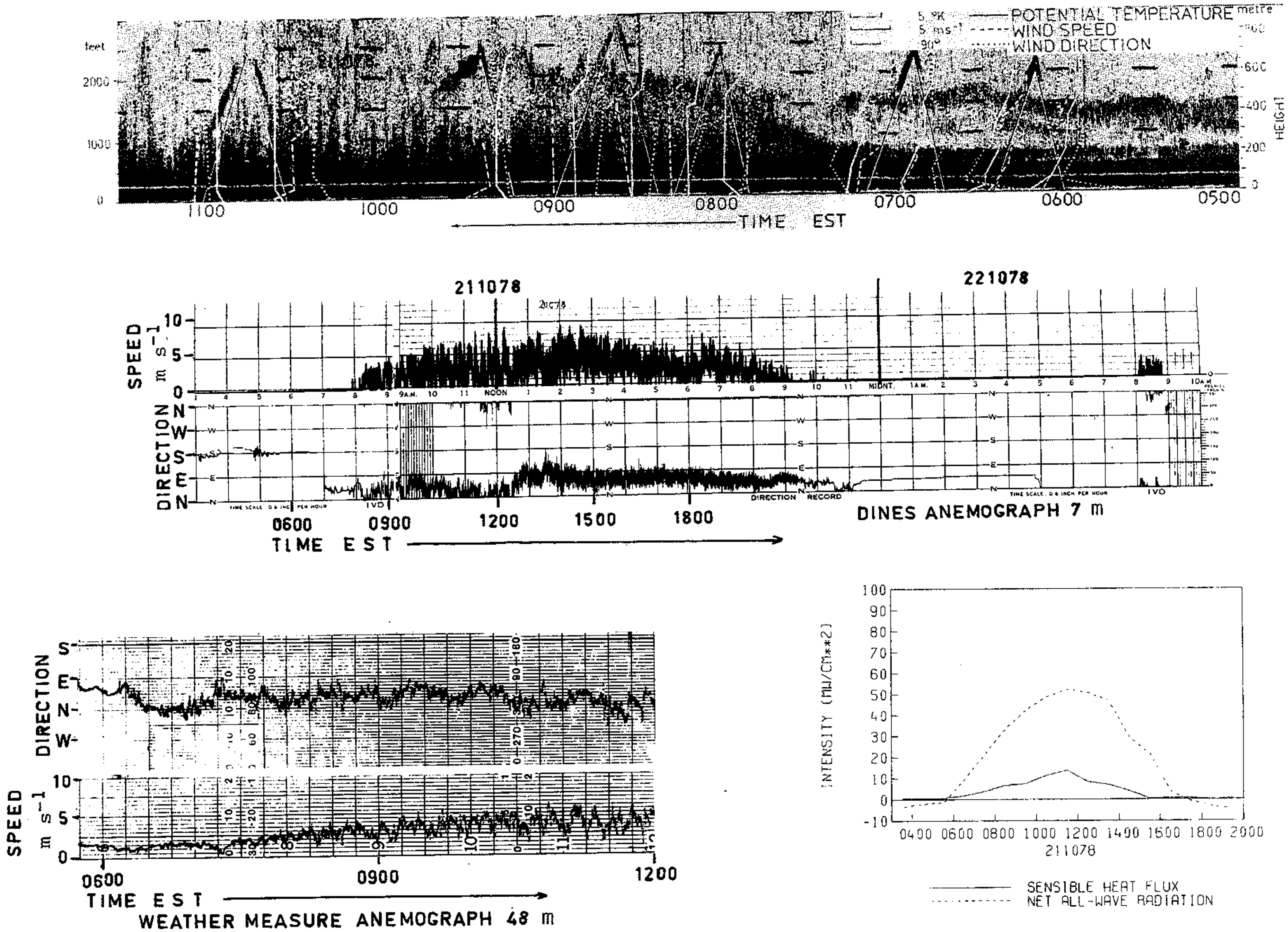


FIGURE 11. METEOROLOGICAL AND ACOUSTIC SOUNDER DATA - ATMOSPHERIC MIXING LAYER DEVELOPMENT, 21 OCTOBER 1978

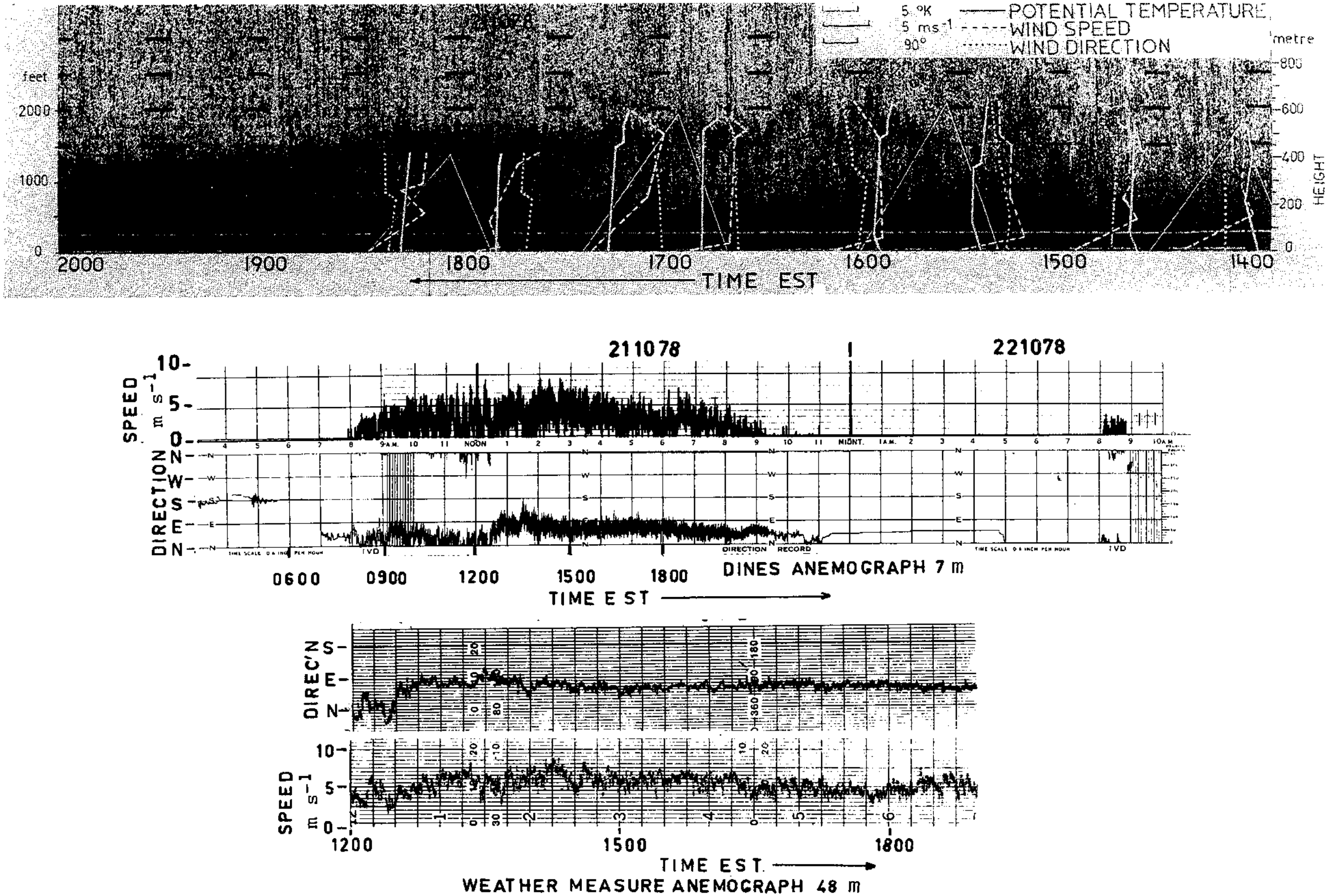


FIGURE 12. METEOROLOGICAL AND ACOUSTIC SOUNDER DATA - EAST-NORTH-EAST SEA BREEZE WIND REGIME, 21 OCTOBER 1978

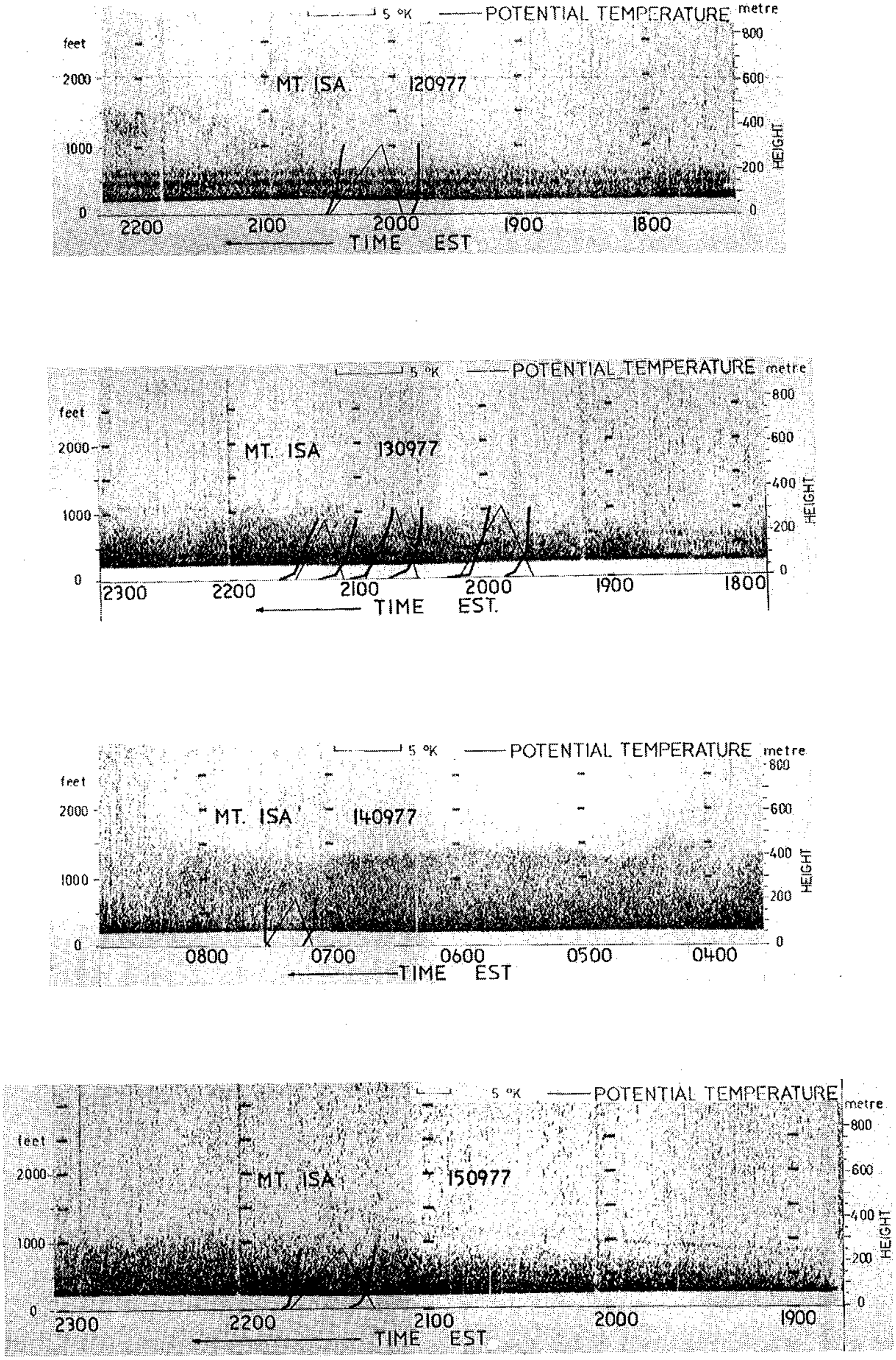


**FIGURE 13. Mt. ISA ACOUSTIC SOUNDER AND METEOROLOGICAL DATA, 12 TO 15 SEPTEMBER 1977**

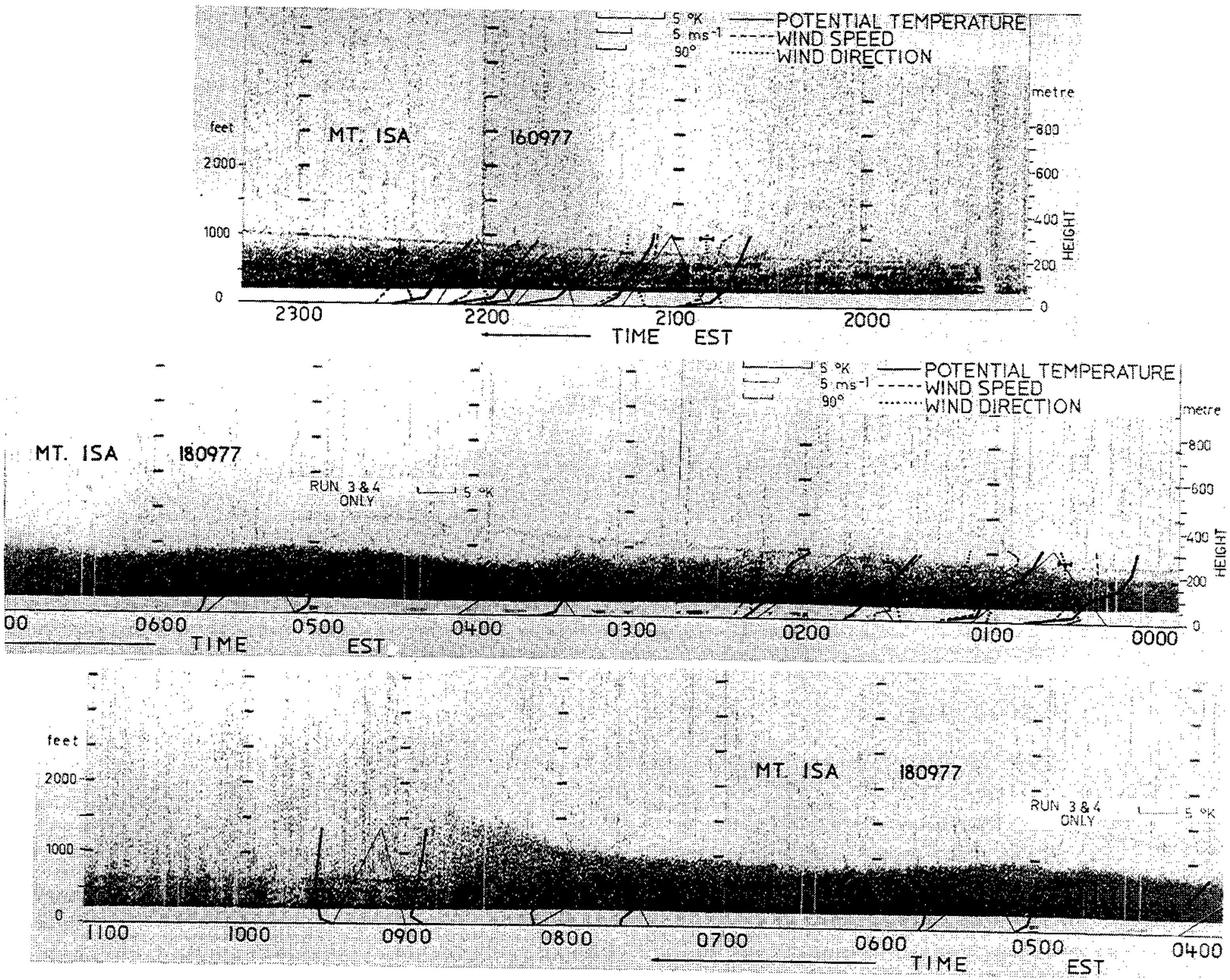


**FIGURE 14. Mt. ISA ACOUSTIC SOUNDER AND METEOROLOGICAL DATA, 16 AND 18 SEPTEMBER 1977**

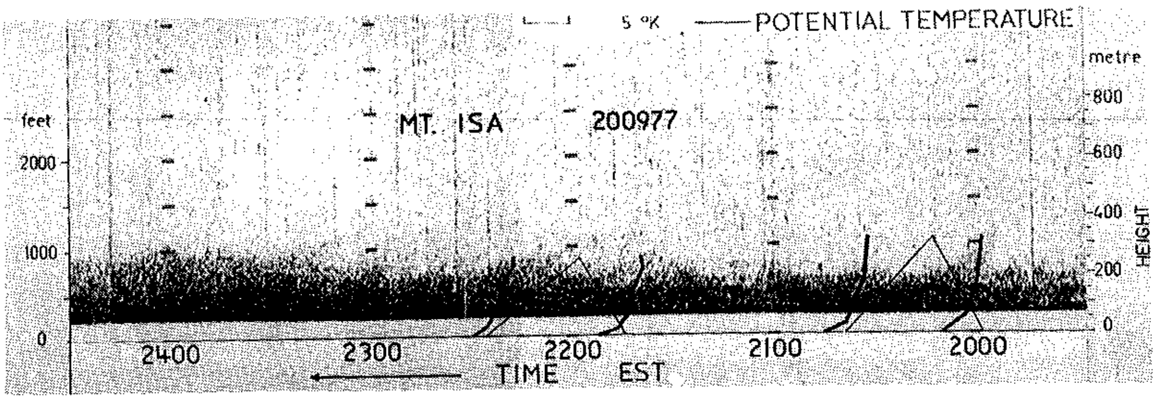


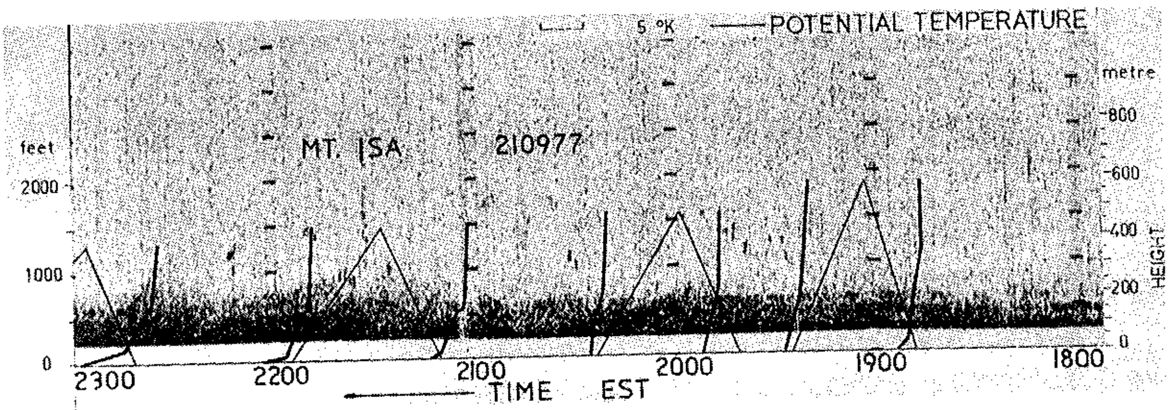


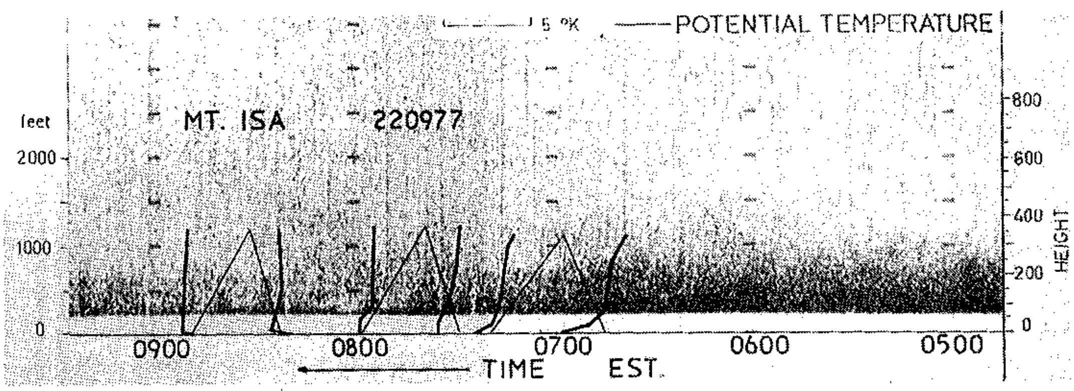


**FIGURE 15. Mt. ISA ACOUSTIC SOUNDER AND METEOROLOGICAL DATA, 20 TO 22 SEPTEMBER 1977**

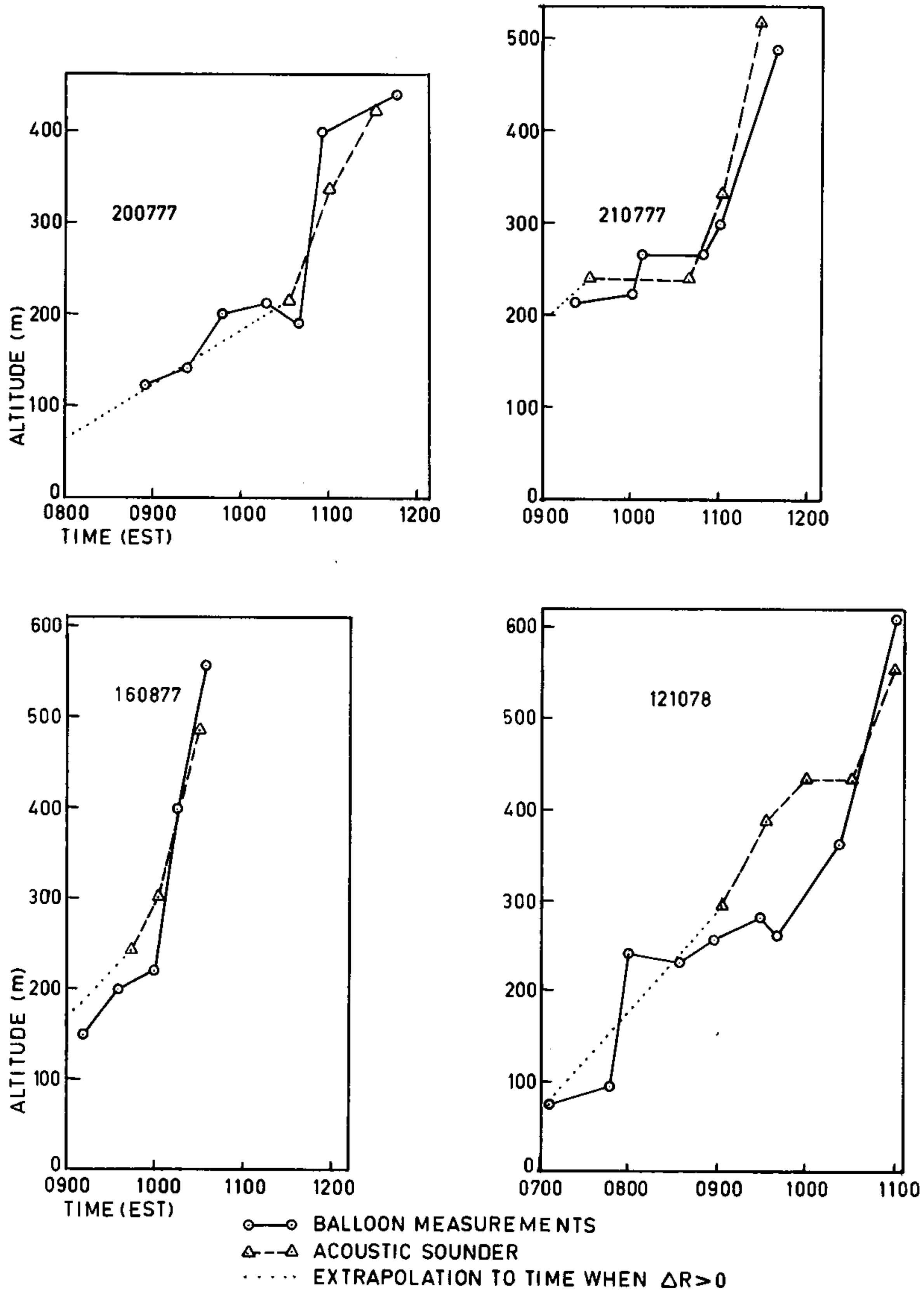


**FIGURE 16. ATMOSPHERIC MIXING LAYER DEVELOPMENT, BALLOON AND ACOUSTIC SOUNDER MEASUREMENTS**

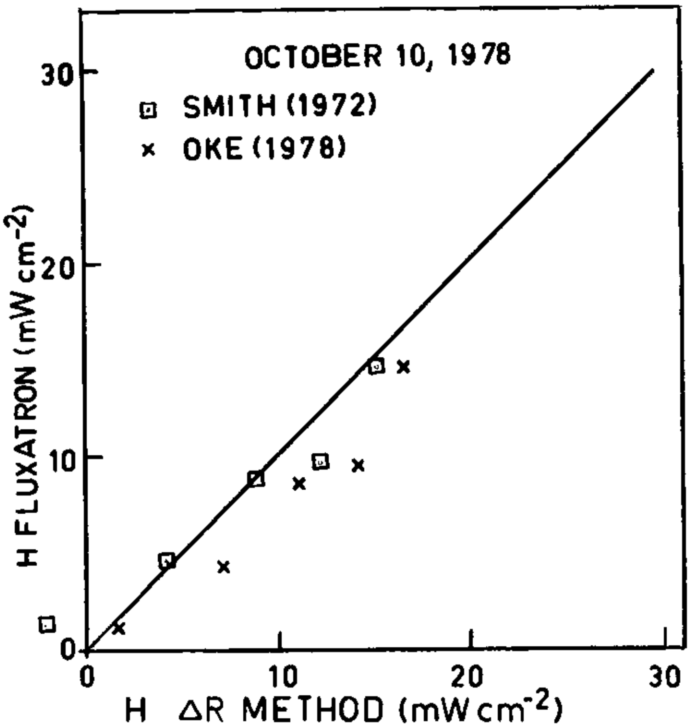


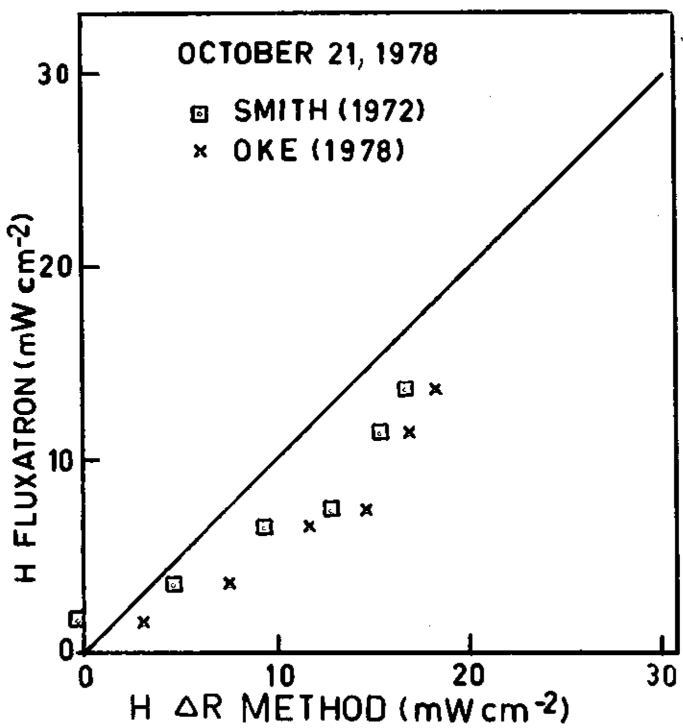


FIGURE 17. COMPARISON OF FLUXATRON, SMITH (1972) AND OKE (1978) VERTICAL SENSIBLE HEAT FLUX ESTIMATES

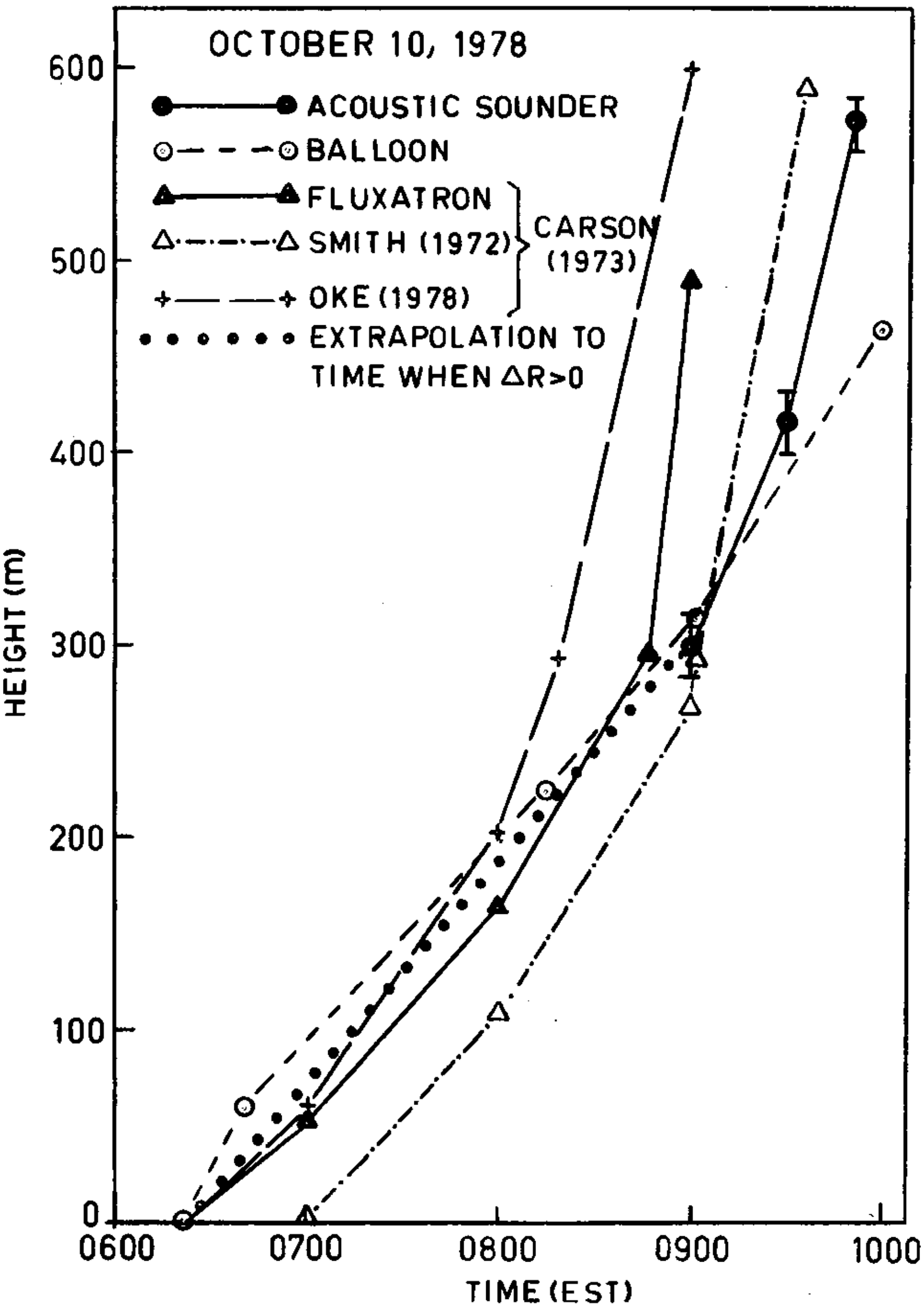


FIGURE 18. COMPARISON OF BALLOON, ACOUSTIC SOUNDER AND THE SIMPLE CARSON (1973) MODEL FOR ATMOSPHERIC MIXING LAYER DEVELOPMENT, 10 OCTOBER 1978

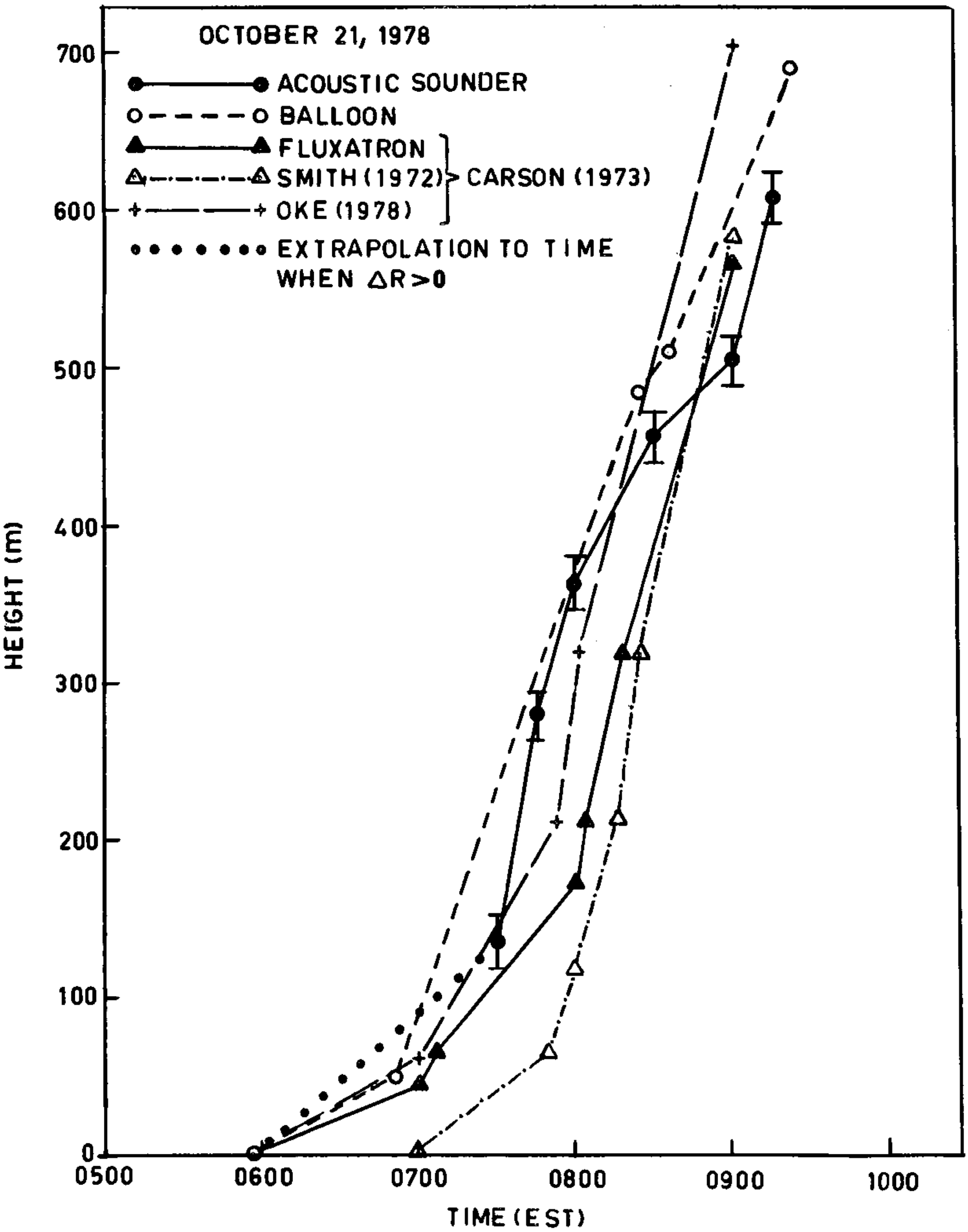


FIGURE 19. COMPARISON OF BALLOON, ACOUSTIC SOUNDER AND THE SIMPLE CARSON (1973) MODEL FOR ATMOSPHERIC MIXING LAYER DEVELOPMENT, 21 OCTOBER 1978

TABLE 1
A COMPARISON OF THE WEATHER MEASURE MARK III AND
DINES PRESSURE TUBE ANEMOMETER RESPONSE CHARACTERISTICS

| | Speed | Direction | | |
|---|---|---|---|---|
| | Threshold ($m\ s^{-1}$) | Threshold ($m\ s^{-1}$) | Distance Constant (m) | Damping Ratio |
| Weather Measure Mark III | 0.34 | 0.34 | 2.4 | 0.4 to 0.6 |
| Dines pressure tube anemograph | > 1.56 | 0.53 | 13.8 | 0.31 to 0.55 |

TABLE 2
SUMMARY OF MT ISA METEOROLOGICAL/ACOUSTIC SOUNDER STUDIES

| Date and Times | Pattern Type Clark et al. [1977] | Prevailing Meteorology and Atmospheric Dispersion Conditions | | |
|---|---|---|---|---|
| | | $\frac{\partial\theta}{\partial z}$(K/100 m) | $\frac{\partial u}{\partial z}$($m\ s^{-1}$/100 m) | Pasquill category* |
| 12 September 1977 | 3 | 0.08 | 1.8 | E |
| 13 September 1977 | 3 | 0.36 | 1.8 | E |
| 14 September 1977 | 4 | 0.33 | 2.7 | E |
| 15 September 1977 | 1 | 0.95 | 2.9 | E |
| 16 September 1977 | 3 | 0.92 | 1.9 | E |
| 18 September 1977 | | | | |
| 0000 to 0215 EST | 3 | 1.55 | 1.6 | F |
| 0215 to 0800 EST | 2 | 1.8 | 3.9 | F |
| 0800 to 0845 EST | 9 | 0.0 | 0.0 | D |
| 20 September 1977 | 3 | 0.8 | 2.0 | E |
| 21 September 1977 | 3 | 0.18 | 1.0 | E |
| 22 September 1977 | 4 | 0.3 | 3.1 | E |

* The classification of the Pasquill stability category is based on USNRC [1972]